UNIVERSITÀ DEGLI STUDI DI MILANO

FACOLTÀ DI SCIENZE E TECNOLOGIE

Corso di Laurea Triennale in Fisica

Tight-binding matrices of graphene nanocones: spectral properties and combinatorics

Relatore:
Prof. Luca Guido A. Molinari
Correlatore:
Prof. Stefano Evangelisti

Candidato:
Mattia Carrozzo
Matricola: 874413

Anno Accademico 2020/2021

Abstract

Physics often entails beautiful mathematics, and graphene nanocones are no exception. In this paper, the tight-binding matrices of honeycomb triangles and trapezia are investigated, and intriguing mathematical features of their determinants are uncovered. In particular, three identities for the Hückel determinant are conjectured, involving permanents and Pascal matrices, or variants of them, with binomial coefficients as their elements. This establishes connections with counting problems in statistical mechanics and has implications in theoretical chemistry.

Contents

Introduction

Graphene[1–4] (Fig. 1c) is an allotrope of carbon consisting of a single layer of atoms bound together in a chicken-wire pattern of hexagons, and exhibits fascinating properties arising from its two-dimensional honeycomb lattice nanostructures. In fact, it can be considered to be a basic block for constructing graphitic materials of all other dimensionalities:[2,3] it can be wrapped up into 0D fullerenes (Fig. 1a), rolled into 1D nanotubes (Fig. 1b) or stacked into 3D graphite (Fig. 1d). Other noteworthy graphene structures are nanocones, nanoflakes and nanoribbons.

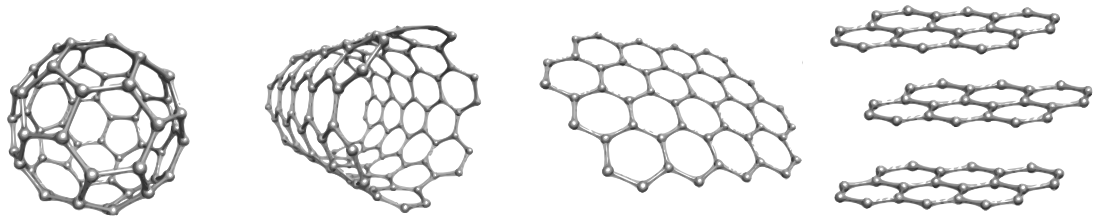

(a) 0D (b) 1D (c) 2D (d) 3D

Figure 1: **Structural models of graphitic nanomaterials.** From left to right: C_{60} fullerene, a carbon nanotube, graphene and graphite (Susi,[5] 2015).

Brief history of graphene Graphene has likely been unconsciously produced in small quantities for centuries, through the use of pencils and other similar applications of graphite.[3] Theoretically, it has been studied for decades, and widely used to describe features of various other carbon-based materials.
On the other hand, graphene was presumed not to exist as a free-standing material and believed to be thermodynamically unstable[2] with respect to the formation of curved structures such as fullerenes and nanotubes. But all of a sudden, the "impossible" material turned into reality when, in 2004, it was properly isolated and characterized by Andre Geim and Konstantin Novoselov at the University of Manchester. They pulled graphene layers from a lump of graphite with a common adhesive tape, using a process of mechanical exfoliation called either *micromechanical cleavage* or the *Scotch tape technique*.

Their simple but ingenious idea resulted in the Nobel Prize in Physics in 2010 for their «groundbreaking experiments regarding the two-dimensional material graphene».[6] Their publication, and the surprisingly easy preparation method that they provided, sparked an actual "graphene rush", which is still ongoing: research has expanded and split off into many different subfields, exploring the countless extraordinary properties of the "wonder material".

The wonder material Among the things that make graphene so special, its electronic behaviour is definitely one of the most remarkable. Each carbon atom in a graphene sheet is connected to its three nearest neighbours by a σ-bond,[3] and contributes one electron to a conduction band that extends over the whole sheet. These conduction bands make graphene a zero-gap semimetal with unusual electronic qualities that are better explained by theories for massless relativistic particles rather than the Schrödinger equation.[2] In fact, the interaction beetween the charge carriers and the periodic potential of graphene's honeycomb lattice gives rise to new quasiparticles that show linear, rather than quadratic, dependence of energy on momentum, and are accurately described by the Dirac equation, with an effective speed of light $v_F \approx 10^6 \mathrm{m/s}$.[2,3] These quasiparticles, called *massless Dirac fermions*,[3] can be seen either as electrons that lost their rest mass m_0, or as neutrinos that gained the electron charge e, and provide a new way to probe quantum electrodynamics phenomena,[2] by mesuring graphene's electronic properties.
Furthermore, graphene conducts heat better than diamond and electricity better than silver, and it is also about 200 times stronger than would be the strongest steel of the same thickness.[1,7] It strongly absorbs light of all visible wavelengths, which accounts for the black color of graphite; yet a single graphene sheet is nearly transparent because of its extreme thinness. The material is also impermeable, flexible and incredibly light, and exhibits several other outstanding qualities[7] on which we will not dwell.

A chicken-wire-like future All these exceptional properties make graphene a unique material, not only from the point of view of fundamental physics, but also for its potentially profitable applications.
Despite its short history, it has rapidly become a valuable and useful nanomaterial with a global market worth millions of dollars.[7] In fact, along with some new considerable challenges, graphene has brought great promises, including high-performance semiconductors, more efficient electric batteries, and even a space elavator,[8] which would eventually turn out to be the most ambitious human engineering work of all time.

In this paper we investigate the matrices of graphene nanocones and nano-conical-frusta (truncated nanocones), in a tight-binding approximation. In particular, we uncover intriguing mathematical features regarding the Hückel determinant and conjecture identities involving the Pascal matrix and related ones, with binomial coefficients as matrix elements.
To achieve this purpose, we consider honeycomb triangles and trapezia with $n+1$ rows

and Bloch boundary conditions at the end of each row. It is deemed convenient to replace the phase factors $e^{\pm i\theta}$ with two free parameters x and y, or by parameters $(\mathbf{x}, \mathbf{y})$ where $\mathbf{x} = (x_0, ..., x_n)$ and $\mathbf{y} = (y_0, ..., y_n)$.
The manuscript is organized in three chapters: in the first one we introduce the preliminary concepts, necessary to contextualize this work; the second chapter is dedicated to the conjectures, while in the third one we discuss results and future directions.

Chapter 1

Preliminary concepts

In this first chapter we discuss the basic elements and provide the essential definitions that will contribute to build a coherent theoretical framework. Moreover, we include useful examples and figures, for a better fruition by the readers. Finally, we dedicate a small section to contextualize the present work, mentioning the circumstances and the ideas that first encouraged it.

1.1 Graphene nanocones

In the final analysis, one might say that graphene's greatest blessing lies in its element: the unique ability of carbon[9] in forming strong covalent bonds to construct stable and highly symmetrical geometries, is at the basis of the entire nanotechnology industry, organic chemistry, and eventually of life itself.
As hinted in the Introduction, a carbon atom can be thought as a basic building unit for a vast variety of topologies: starting from a graphene sheet, one can obtain non-planar structures by introducing polygonal defects that provide the curvature. For instance, pentagonal defects in the two-dimensional graphitic network produce fullerene, which, wrapped around itself, looks essentially zero-dimensional.[2,3,9]
Among all the countless carbon edifices, some received less attention than others:[9,10] this is the case of graphene nanocones (Fig. 1.2). Despite the fact that they have been observed[11,12] just after the discovery of nanotubes in 1991, these conical constructions have just recently started attracting a considerable interest, due to their relatively easy preparation method and many other peculiar properties that make them a scientifically and technologically relevant class of nanostructures.[9]

Consider a nearly perfect monolayer of graphite: if from the center of a graphene hexagon, we draw six lines that bisect the sides (Fig. 1.1a), we obtain six triangles with a carbon atom of the hexagon at the tip, and rows of 1, 2, 3, ... hexagons. If five such triangles

are rejoined by connecting lateral bonds, a conical honeycomb surface is obtained (Figs. 1.1b and 1.1c), with a pentagon at the top and rings of 5, 10, 15, ... hexagons. The apex angle of this infinite nanocone is about 113°, the largest possible aperture for this class of nanostructures. In Corannulene, $C_{20}H_{10}$, the pentagon is surrounded by a single ring of five carbon hexagons (to which, from now on, we will also refer as *benzenoids*), with ten hydrogen atoms attached to. It has the shape of a bowl, that can invert concavity by thermal activation.

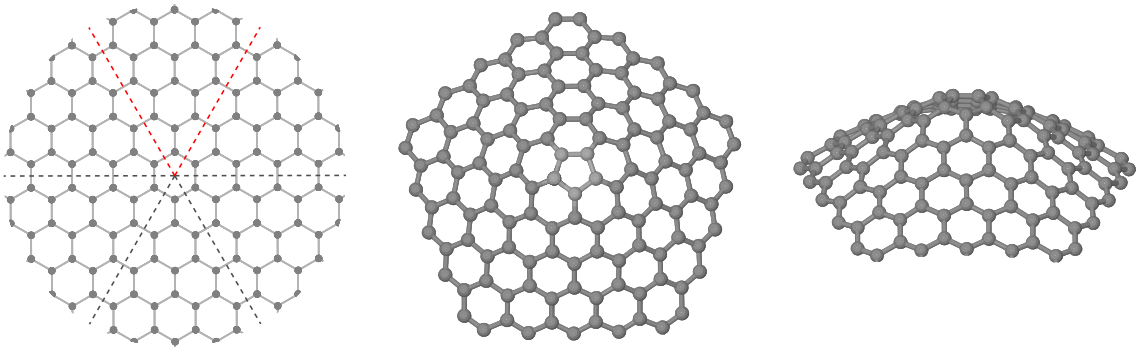

(a) top view (b) top view (c) side view

Figure 1.1: **Rise of a graphene nanocone.** The extraction of a 60° wedge from a graphene sheet(a), leads to the formation of a conical structure (b, c) by incorporation of a single pentagonal defect in the hexagonal network (Figs. b and c by Evangelisti,[13] 2021).

Finite nanocones have several rings of benzenoids, covering a conical surface. The cap may consist of a "carbon polygon" with a number of vertices from 1 to 5, causing five different cone apertures, according to which the nanocones are classified. Those with smallest angle, around 19°, were synthetized for the first time by Ge and Sattler in 1994,[11] in the hot vapour phase of carbon. The other types, corresponding to cone angles of 39°, 60°, 85° and 113° were found by accident, under pyrolysis of hydrocarbons.[14,15] It can be proved[10,11] that only these five classes of cones can be obtained from a single continuous graphitic sheet. The typical length of a graphene nanocone is some tens of nanometers, corresponding to order 10^8 carbon atoms, while inter lattice spacing is of a few ångströms.
The simplest approach to such structures is the tight-binding approximation. The tight-binding Hamiltonian is a topological matrix named after Erich Hückel. Chemists parametrize the Hückel matrix in the following way:

$$H_{ij} = \begin{cases} \alpha & i = j \\ \beta & i, j \text{ adjacent} \\ 0 & \text{otherwise} \end{cases}$$

where α and β are tight-binding parameters that depends on the atoms involved.

The symmetry C_n of nanocones restricts the Hamiltonian to a single triangle with Bloch boundary conditions on two sides.[15]

We give the following operational definitions:

Definition 1.1.1. A graphene nanocone of size n, is the conical surface formed by n rings of benzenoids, where n is a positive integer.

Definition 1.1.2. Given a graphene nanocone of size n, a truncated nanocone (or conical frustum) of size $n - k$, is the structure obtained by removing the first k rings from the nanocone, with $0 \leq k \leq n$.

According to these intuitive definitions, it is trivial that a graphene truncated cone can be seen as a generalization of a nanocone, to which the frustum is reduced in the case $k = 0$.

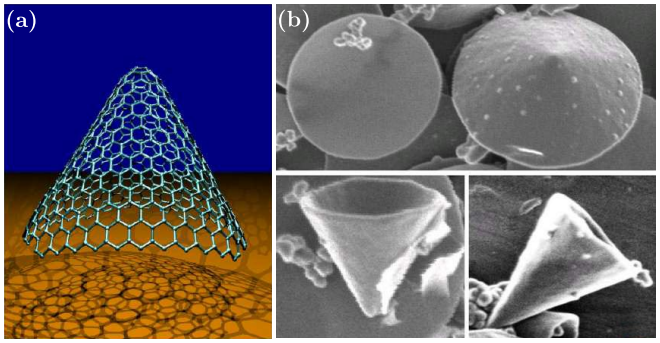

Figure 1.2: **Graphene nanocones.** (a) Computer model of a graphene nanocone (Terrones,[16] 2003). (b) Scanning electron microscope images of carbon nanocones (diameter $\sim 1\mu$m) produced in the Kvaerner Carbon Black & Hydrogen Process (Knudsen, 2010).

1.2 Graphene triangles and trapezia

For our purposes, it is convenient to deal with 2D honeycomb triangles and trapezia, rather than 3D nanocones and conical frusta. In fact, by exploiting the discrete rotational symmetry of nanocones, we can just obtain the information from one of the equivalent triangles in Fig. 1.1a and then, under proper Bloch boundary conditions, merge them together to get the original conical structure. Obviously, the same applies for truncated nanocones and trapezia.
For the sake of generality, in this discussion we will refer, as much as possible, to triangles and trapezia of generic size n, leaving those with specific size for purely illustrative examples.

Although graphene triangles were already introduced earlier, here we provide a more formal characterization:

Definition 1.2.1. A graphene triangle of size n, is a triangle of carbon atoms that consists of $n+1$ rows with 1, 3, ..., $2n+1$ atoms.

Similarly to what happened with nanocones and conical frusta, we have:

Definition 1.2.2. Given a graphene triangle of size n, a graphene trapezium of size $n-k$, is a trapezium of carbon atoms obtained by removing the first k rows from the triangle, with $0 \leq k \leq n$. It is formed by $n-k+1$ rows with $2k+1, 2k+3, ..., 2n+1$ atoms.

1.2.1 The Hückel matrix

At this point, we have all the ingredients to introduce the main subject of this dissertation:

Definition 1.2.3. The Hückel matrix (tight-binding matrix) of a graphene triangle with $n+1$ rows and Bloch parameters $(\mathbf{x}, \mathbf{y})$, is a square block tridiagonal matrix H_n of size $(n+1)^2$ such that:

$$H_n(\mathbf{x},\mathbf{y}) = \begin{bmatrix} T_0 & R_1^\top & & & \\ R_1 & T_1 & R_2^\top & & \\ & R_2 & \ddots & \ddots & \\ & & \ddots & & R_{n-1}^\top \\ & & & R_{n-1} & T_n \end{bmatrix}$$

Example 1.2.1. *Hückel matrix of a honeycomb triangle with 5 rows and associated graph:*

$$H_4(\mathbf{x},\mathbf{y}) = \begin{bmatrix} T_0 & R_1^\top & & & \\ R_1 & T_1 & R_2^\top & & \\ & R_2 & T_2 & R_3^\top & \\ & & R_3 & T_3 & R_4^\top \\ & & & R_4 & T_4 \end{bmatrix}$$

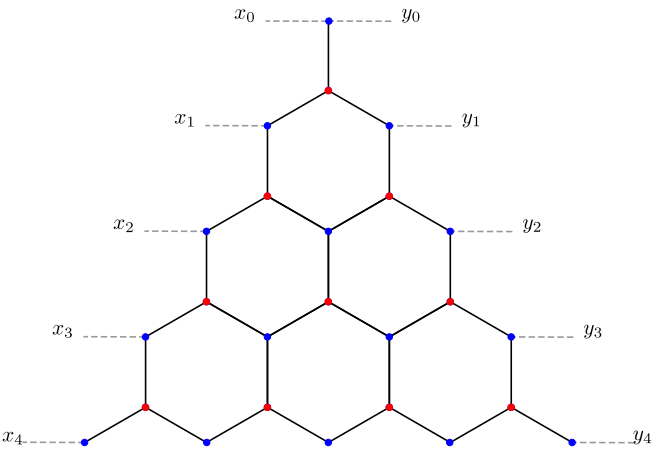

The diagonal blocks in H_n are square matrices $T_m(x_m, y_m)$ of size $2m+1$ that describe closed chains with nearest-neighbour couplings. They exhibit the following structure:

$$T_m(x_m,y_m) = \begin{bmatrix} 0 & 1 & & y_m \\ 1 & \ddots & \ddots & \\ & \ddots & & 1 \\ x_m & & 1 & 0 \end{bmatrix} \quad \begin{matrix} \overset{2m+1}{\longleftrightarrow} \\ \\ \\ \\ \updownarrow 2m+1 \end{matrix}$$

Example 1.2.2. 5×5 *matrix* T_2 *with its graph:*

$$T_2(x_2, y_2) = \begin{bmatrix} 0 & 1 & & & y_2 \\ 1 & 0 & 1 & & \\ & 1 & 0 & 1 & \\ & & 1 & 0 & 1 \\ x_2 & & & 1 & 0 \end{bmatrix}$$

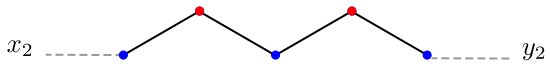

Links in the graph are represented by non-zero matrix elements $T_{i,i+1} = T_{i+1,i} = 1$; the extremal dots are also connected by a (dotted) link with directional weights $T_{2m+1,1} = x_m$ and $T_{1,2m+1} = y_m$. It is $T_0(x_0, y_0) = x_0 + y_0$.
Besides, for any odd size 2m + 1, the following relation holds:

$$\det T_m(x_m, y_m) = x_m + y_m$$

The off diagonal rectangular matrices R_m, together with their transpose $R_m^\top$, represent the link between matrices T_{m-1} and T_m; they have size $(2m+1) \times (2m-1)$ and structure:

$$R_m = \overset{\longleftarrow 2m-1 \longrightarrow}{\begin{bmatrix} 0 & 0 & 0 & 0 & 0 & \dots & 0 \\ 1 & & & & & & \\ & 0 & & & & & \\ & & 1 & & & & \\ & & & \ddots & & & \\ & & & & 1 & & \\ & & & & & 0 & \\ & & & & & & 1 \\ 0 & 0 & 0 & 0 & 0 & \dots & 0 \end{bmatrix}} \quad \updownarrow 2m+1$$

Example 1.2.3. *Matrices* R_m *and their transpose for* $m = 1, 2, 3$:

$$R_1 = \begin{bmatrix} 0 \\ 1 \\ 0 \end{bmatrix} \qquad R_2 = \begin{bmatrix} 0 & 0 & 0 \\ 1 & & \\ & 0 & \\ & & 1 \\ 0 & 0 & 0 \end{bmatrix} \qquad R_3 = \begin{bmatrix} 0 & 0 & 0 & 0 & 0 \\ 1 & & & & \\ & 0 & & & \\ & & 1 & & \\ & & & 0 & \\ & & & & 1 \\ 0 & 0 & 0 & 0 & 0 \end{bmatrix}$$

$$R_1^\top = \begin{bmatrix} 0 & 1 & 0 \end{bmatrix} \quad R_2^\top = \begin{bmatrix} 0 & 1 & & 0 \\ 0 & & 0 & 0 \\ 0 & & 1 & 0 \end{bmatrix} \quad R_3^\top = \begin{bmatrix} 0 & 1 & & & 0 \\ 0 & & 0 & & 0 \\ 0 & & & 1 & 0 \\ 0 & & & 0 & 0 \\ 0 & & & & 1 & 0 \end{bmatrix}$$

The unit matrix elements in R_m and $R_m^\top$ are the vertical links in the graph of H_n, joining a dot in row $m-1$ and a dot in row m.

The size of the matrix H_n is $N = 1+3+\cdots+(2n-1)+(2n+1) = (n+1)^2$.

Example 1.2.4. 9×9 *matrix* H_2 *and related graph:*

$$H_2 = \left[\begin{array}{c|ccc|cccc} x_0+y_0 & 0 & 1 & 0 & & & & \\ \hline 0 & 0 & 1 & y_1 & 0 & 1 & & 0 \\ 1 & 1 & 0 & 1 & 0 & & 0 & 0 \\ 0 & x_1 & 1 & 0 & 0 & & 1 & 0 \\ \hline & 0 & 0 & 0 & 0 & 1 & & y_2 \\ & 1 & & & 1 & 0 & 1 & \\ & & 0 & & & 1 & 0 & 1 \\ & & & 1 & & & 1 & 0 & 1 \\ & 0 & 0 & 0 & x_2 & & & 1 & 0 \end{array}\right]$$

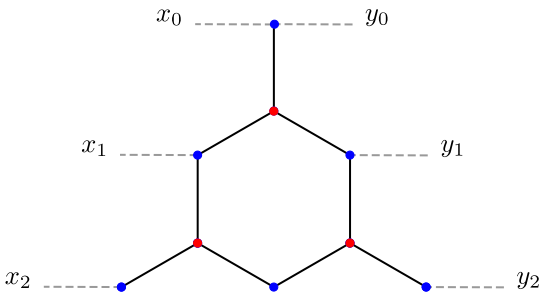

Therefore, the graph of a Hückel matrix $H_n(\mathbf{x},\mathbf{y})$ of size N can be described as a set of vertices $1,2,...,N$ with edges that connect vertex j and vertex k whenever $H_{jk}\neq 0$. It displays the nonzero matrix elements $H_{ij} = H_{ji} = 1$ as a non-oriented edge among vertices i and j. The rows, with oblique edges, are the graphs of matrices $T_m(x_m,y_m)$, while the vertical edges represent the nonzero matrix elements of R_m and $R_m^\top$; extremal vertices of each row are connected by a dotted oriented edge, with weight x_m from left to right and y_m from right to left (Ex. 1.2.2).
The number of vertices is $N = (n+1)^2$; the number of oblique and vertical edges is $n(n+1)$ and $\frac{n}{2}(n+1)$, respectively, while that of dotted edges is $n+1$ (one edge is the loop of vertex 1 with itself); finally, the total number of edges is $\frac{n+1}{2}(3n+2)$.

When $x_m = y_m = 1\ \forall m : 0\le m\le n$, the Hückel matrix H_n is almost doubly stochastic:[17] the sum of rows and columns is equal to 3, with the exception of $n+1$ rows and columns, where the sum is 2. The addition of a block $J_n = \mathrm{diag}[1,0,1,...,1]$ to T_n makes H_n doubly stochastic, thus a convex combination of permutation matrices (Birkhoff's theorem).

Allow us to spend a few words on the Hückel matrices of trapezia.

Definition 1.2.4. Given a honeycomb triangle with Hückel matrix H_n, the Hückel matrix of a honeycomb trapezium with $n-k+1$ rows and Bloch parameters $(\mathbf{x},\mathbf{y})$, is a square block tridiagonal matrix $H_{k,n}$, obtained from the matrix H_n by deleting the first k^2 rows and columns. It has size $N = (2k+1)+(2k+3)+\cdots+(2n+1) = (n+1)^2-k^2$ and the following structure:

$$H_{k,n}(\mathbf{x},\mathbf{y}) = \begin{bmatrix} T_k & R_{k+1}^\top & & & \\ R_{k+1} & T_{k+1} & R_{k+2}^\top & & \\ & R_{k+2} & \ddots & \ddots & \\ & & \ddots & & R_{n-1}^\top \\ & & & R_{n-1} & T_n \end{bmatrix}$$

Example 1.2.5. 21×21 *matrix* $H_{2,4}$ *with its graph:*

$$H_{2,4}(\mathbf{x},\mathbf{y}) = \begin{bmatrix} T_2 & R_3^\top & \\ R_3 & T_3 & R_4^\top \\ & R_4 & T_4 \end{bmatrix}$$

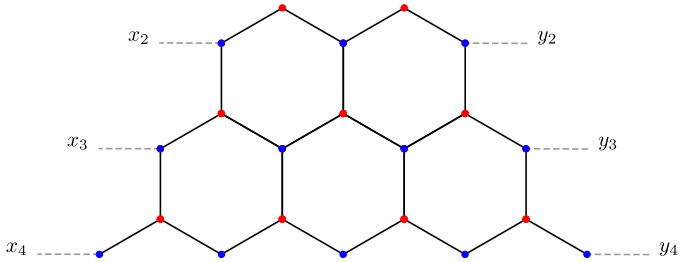

From Defs. 1.2.1 and 1.2.2 it is straightforward that $H_{0,n} = H_n$ and $H_{n,n} = T_n$.

1.2.2 The Hückel determinant

The determinants of the first Hückel matrices, with Bloch parameters x and y, are numerically evaluated*, both for honeycomb triangles and trapezia:

$$\det H_0 = x + y$$
$$\det H_1 = x^2 + 3xy + y^2$$
$$\det H_2 = x^3 + 9x^2y + 9xy^2 + y^3$$
$$\det H_3 = x^4 + 29x^3y + 72x^2y^2 + 29xy^3 + y^4$$
$$\det H_4 = x^5 + 99x^4y + 626x^3y^2 + 626x^2y^3 + 99xy^4 + y^5$$
$$\det H_5 = x^6 + 351x^5y + 6084x^4y^2 + 13869x^3y^3 + 6084x^2y^4 + 351xy^5 + y^6$$
$$\det H_6 = x^7 + 1275x^6y + 64974x^5y^2 + 347020x^4y^3 + 347020x^3y^4 + 64974x^2y^5 + 1275xy^6 + y^7$$

$$\det H_{7,7} = x + y$$
$$\det H_{6,7} = x^2 + 51xy + y^2$$
$$\det H_{5,7} = x^3 + 529x^2y + 529xy^2 + y^3$$
$$\det H_{4,7} = x^4 + 2005x^3y + 23608x^2y^2 + 2005xy^3 + y^4$$
$$\det H_{3,7} = x^5 + 3747x^4y + 203402x^3y^2 + 203402x^2y^3 + 3747xy^4 + y^5$$
$$\det H_{2,7} = x^6 + 4559x^5y + 544100x^4y^2 + 2614205x^3y^3 + 544100x^2y^4 + 4559xy^5 + y^6$$
$$\det H_{1,7} = x^7 + 4699x^6y + 719406x^5y^2 + 7688684x^4y^3 + 7688684x^3y^4 + 719406x^2y^5 + 4699xy^6 + y^7$$

*For these and other numerical computations, a version of Wolfram Mathematica 12 Student Edition was used.

The evaluations show the interesting fact that all coefficients are positive, and other features that will be proven in general.
In particular, by iterating Schur's reduction for block matrices (see Appendix A), it was found[17] that the determinant of a Hückel matrix of size $(n+1)^2$ shrinks to the determinant of a matrix of size $n+1$, with binomial coefficients. Lunnon's paper[18] gave the hint that Hückel determinants are characteristic polynomials of the symmetric Pascal matrices.
Before embarking in the study of Hückel determinants of honeycomb triangles and trapezia, let us introduce Pascal matrices in an appropriate way.

1.3 Pascal matrices

The Pascal matrix is a square matrix containing the binomial coefficients of Pascal's triangle as its elements, and there is a vast literature about it.[18–20] In the next chapter, we will unveil a truly surprising relation involving these matrices, while here we limit ourselves to recalling some relevant facts around them.

The magical patterns of Pascal's triangle have enchanted mathematicians since the dawn of time.[21] It can be represented as a square matrix in three different ways: as either a lower-triangular, an upper-triangular, or a full, symmetric matrix. The $(n+1)\times(n+1)$ lower-triangular matrix P_n has nonzero elements given by $(P_n)_{ij} = \binom{i}{j}$, $j \le i$. Its 5×5 truncation is shown below:

Example 1.3.1. *Lower-triangular Pascal matrix P_4:*

$$P_4 = \begin{bmatrix} \binom{0}{0} & & & & \\ \binom{1}{0} & \binom{1}{1} & & & \\ \binom{2}{0} & \binom{2}{1} & \binom{2}{2} & & \\ \binom{3}{0} & \binom{3}{1} & \binom{3}{2} & \binom{3}{3} & \\ \binom{4}{0} & \binom{4}{1} & \binom{4}{2} & \binom{4}{3} & \binom{4}{4} \end{bmatrix} = \begin{bmatrix} 1 & & & & \\ 1 & 1 & & & \\ 1 & 2 & 1 & & \\ 1 & 3 & 3 & 1 & \\ 1 & 4 & 6 & 4 & 1 \end{bmatrix}$$

Unsurprisingly, the transpose matrix of P_n is the corresponding upper-triangular Pascal matrix, with nonzero elements $(P_n^\top)_{ij} = \binom{j}{i}$, $i \le j$.

Example 1.3.2. 5×5 *upper-triangular Pascal matrix $P_4^\top$:*

$$P_4^\top = \begin{bmatrix} \binom{0}{0} & \binom{1}{0} & \binom{2}{0} & \binom{3}{0} & \binom{4}{0} \\ & \binom{1}{1} & \binom{2}{1} & \binom{3}{1} & \binom{4}{1} \\ & & \binom{2}{2} & \binom{3}{2} & \binom{4}{2} \\ & & & \binom{3}{3} & \binom{4}{3} \\ & & & & \binom{4}{4} \end{bmatrix} = \begin{bmatrix} 1 & 1 & 1 & 1 & 1 \\ & 1 & 2 & 3 & 4 \\ & & 1 & 3 & 6 \\ & & & 1 & 4 \\ & & & & 1 \end{bmatrix}$$

The inverse matrix of P_n has the same binomial elements, but with alternating signs. This property arises from the following inversion theorem:[17]

$$a_n = \sum_{k=0}^{n} \binom{n}{k} b_k \Rightarrow b_n = \sum_{k=0}^{n} (-1)^k \binom{n}{k} a_k$$

Example 1.3.3. *Inverse matrix of* P_4*:*

$$P_4^{-1} = \begin{bmatrix} \binom{0}{0} & & & & \\ -\binom{1}{0} & \binom{1}{1} & & & \\ \binom{2}{0} & -\binom{2}{1} & \binom{2}{2} & & \\ -\binom{3}{0} & \binom{3}{1} & -\binom{3}{2} & \binom{3}{3} & \\ \binom{4}{0} & -\binom{4}{1} & \binom{4}{2} & -\binom{4}{3} & \binom{4}{4} \end{bmatrix} = \begin{bmatrix} 1 & & & & \\ -1 & 1 & & & \\ 1 & -2 & 1 & & \\ -1 & 3 & -3 & 1 & \\ 1 & -4 & 6 & -4 & 1 \end{bmatrix}$$

It has been proved[19] that the product $P_n P_n^\top$ is the Cholesky factorization of the symmetric Pascal matrix Q_n, that displays binomial elements $(Q_n)_{ij} = \binom{i+j}{j}$, with $i, j = 0, ..., n$.

Example 1.3.4. 5×5 *symmetrical Pascal matrix* Q_4*:*

$$Q_4 = \begin{bmatrix} 1 & & & & \\ 1 & 1 & & & \\ 1 & 2 & 1 & & \\ 1 & 3 & 3 & 1 & \\ 1 & 4 & 6 & 4 & 1 \end{bmatrix} \begin{bmatrix} 1 & 1 & 1 & 1 & 1 \\ & 1 & 2 & 3 & 4 \\ & & 1 & 3 & 6 \\ & & & 1 & 4 \\ & & & & 1 \end{bmatrix} = \begin{bmatrix} 1 & 1 & 1 & 1 & 1 \\ 1 & 2 & 3 & 4 & 5 \\ 1 & 3 & 6 & 10 & 15 \\ 1 & 4 & 10 & 20 & 35 \\ 1 & 5 & 15 & 35 & 70 \end{bmatrix}$$

From the pleasing relationship $Q_n = P_n P_n^\top$, it is trivial that the symmetric Pascal matrix is positive definite and with unit determinant, since for triangular matrices the determinant is simply the product of their diagonal entries, which are all 1 for both P_n and $P_n^\top$. Moreover, the eigenvalues are strictly positive and come in reciprocal pairs[20,22] $(q, 1/q)$, following from the fact that Q_n is similar to its inverse Q_n^{-1}. Notice that if the size of the matrix is odd (n even), one of the eigenvalues must be equal to 1, since the eigenvalues must come in pairs. As a consequence of positive eigenvalues, the coefficients of the polynomial $\det[z + Q_n]$ are all positive.

Example 1.3.5. *The eigenvalues of the* 2×2 *symmetric Pascal matrix* Q_1 *are* $q_1 = \frac{3+\sqrt{5}}{2}$ *and* $q_2 = \frac{3-\sqrt{5}}{2}$*, where* $q_1 q_2 = 1$ *gives a reciprocal pair.*
Let now the size be equal to 3*; the eigenvalues of the symmetric Pascal matrix* Q_2 *are* $q_1 = 4 + \sqrt{15}$*,* $q_2 = 4 - \sqrt{15}$ *and* $q_3 = 1$*, where* $q_1 q_2 = 1$ *gives a reciprocal pair and* q_3 *is a self-reciprocal.*

An alternative way to construct Pascal matrices could be that of taking the matrix exponential of particular subdiagonal and superdiagonal matrices, as shown in the example below, valid for any $n \times n$ matrices.

Example 1.3.6. 5×5 *Pascal matrices viewed as matrix exponentials:*

$$P_4 = \exp\left(\begin{bmatrix} 0 & & & & \\ 1 & 0 & & & \\ & 2 & 0 & & \\ & & 3 & 0 & \\ & & & 4 & 0 \end{bmatrix}\right) = \begin{bmatrix} 1 & & & & \\ 1 & 1 & & & \\ 1 & 2 & 1 & & \\ 1 & 3 & 3 & 1 & \\ 1 & 4 & 6 & 4 & 1 \end{bmatrix}$$

$$P_4^\top = \exp\left(\begin{bmatrix} 0 & 1 & & & \\ & 0 & 2 & & \\ & & 0 & 3 & \\ & & & 0 & 4 \\ & & & & 0 \end{bmatrix}\right) = \begin{bmatrix} 1 & 1 & 1 & 1 & 1 \\ & 1 & 2 & 3 & 4 \\ & & 1 & 3 & 6 \\ & & & 1 & 4 \\ & & & & 1 \end{bmatrix}$$

Finally, it is interesting to quote the Carlitz matrix $A_n = P_n J_n$, where:

$$J_n = \begin{bmatrix} & & 1 \\ & \iddots & \\ 1 & & \end{bmatrix} \quad \begin{matrix} \overleftarrow{\quad n+1 \quad} \\ \\ \updownarrow n+1 \end{matrix} \qquad J_n^2 = 1 \tag{1.1}$$

Example 1.3.7. 5×5 *Carlitz matrix* A_4 *and its inverse:*

$$A_4 = \begin{bmatrix} & & & & 1 \\ & & & 1 & 1 \\ & & 1 & 2 & 1 \\ & 1 & 3 & 3 & 1 \\ 1 & 4 & 6 & 4 & 1 \end{bmatrix} \qquad A_4^{-1} = \begin{bmatrix} 1 & -4 & 6 & -4 & 1 \\ -1 & 3 & -3 & 1 & \\ 1 & -2 & 1 & & \\ -1 & 1 & & & \\ 1 & & & & \end{bmatrix}$$

Therefore, we can write $A_n A_n^\top = P_n J_n^2 P_n^\top = Q_n$.
The eigenvalues of A_n are the numbers $(-1)^j \phi^{n-2j}$, where $j = 0, ..., n$ and $\phi = \frac{1+\sqrt{5}}{2}$ is the golden ratio.[23]

The Pascal matrices carry all the secrets of the homonymous triangle:[21] from the Fibonacci sequence to the Sierpiński triangle, passing through tetrahedral numbers and powers of eleven, it seems that the whole Number Theory is encoded in their countless patterns. Many of these patterns are stored in the OEIS (*On-Line Encyclopedia of Integer Sequences*), *e.g.* the trace of Q_n for various n (1, 3, 9, 29, 99, 351, 1275, ...) is represented by the sequence A006134.
At this point, to cite Edelman and Strang,[22] it would indeed be «ironic and wonderful» if it turned out that Pascal's triangle is actually applied mathematics.

1.4 The Hückel rule

In this section, we provide a little context and clarify some of the main ideas underlying this project. Standard terms from organic chemistry are used throughout this section; the reader seeking a reference should consult Zhao[24] and Evangelisti.[13]

Aromaticity[24] is a fundamental concept in chemistry, originally introduced to rationalize the exceptional high stability of benzene and related molecules. The term "aromatic" accounts for the intense smell of these compounds and dates back to 1855, when Hofmann used it for the first time.
In 1931, the phisical chemist Erich Hückel provided a theoretical explanation for the aromatic behaviour of benzene and other hydrocarbons, based on approximate molecular orbital (MO) calculations on π electron systems. He showed that the aromaticity of a compound strictly depends on the specific number of delocalized π electrons. This fact was later expressed by Doering with the formula $4n + 2$, and became well known as *Hückel rule*.
More specifically, the rule predicts that planar, monocyclic, completely conjugated hydrocarbons, known as *annulenes*, exhibit aromatic behaviour whenever the total number of electrons in the π system is equal to $4n + 2$, where n is a positive integer.[9] On the contrary, annulenes with $4n$ π electrons are said to be antiaromatic, not to be confused with non-aromatic compounds, which occur when the number is equal to $4n + 1$ or $4n + 3$. For instance, benzene (Fig. 1.3c), with six electrons ($4n + 2$, with $n = 1$), is known to be the most stable among aromatic hydrocarbons, while cyclobutadiene (Fig. 1.3a), with four electrons ($4n$, with $n = 1$), is the only annulene with considerable antiaromaticity.
The higher stability of aromatic systems can be explained in terms of electronic structure properties of their ground state.[9] In fact, according to Huckel's MO theory, $4n + 2$ electrons completely fill all π bonding orbitals, leaving the antibonding ones empty, thus resulting in a wide *HOMO-LUMO gap*[†]. On the other hand, the reason of low stability in antiaromatic rings, lies in the fact that the Fermi level crosses two degenerate non-bonding orbitals, which are only partially occupied by two electrons. This information can be summarized by saying that the ground state wavefunction of aromatic and antiaromatic compounds, manifests a closed-shell (CS) or open-shell (OS) character, respectively.

It is important to point out that Hückel rule, in its original formulation, is only valid for monocyclic hydrocarbons. Therefore, it should not surprise that more general policyclic aromatic hydrocarbons (PAHs), *e.g.* corannulene ($C_{20}H_{10}$), coronene ($C_{24}H_{12}$) and kekulene ($C_{48}H_{24}$), do not fulfill the $4n + 2$ rule.

[†]The acronyms HOMO and LUMO stand for *highest occupied molecular orbital* and *lowest unoccupied molecular orbital*, respectively.

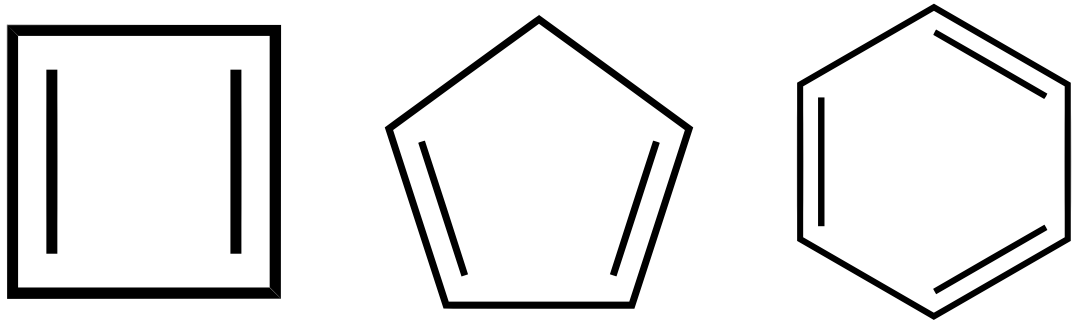

(a) Cyclobutadiene (b) Cyclopentadiene (c) Benzene

Figure 1.3: **Famous monocyclic hydrocarbons.** Benzene (c) and cyclobutadiene (a) are the most aromatic and antiaromatic annulenes, respectively. Although cyclopentadiene (b) is a non-aromatic hydrocarbon, it is popularly used as a precursor to the cyclopentadienyl anion Cp^-, which is the most common anion in organic chemistry and shows aromatic behaviour.

1.4.1 The generalized Hückel rule

In the last decades, many attempts have been made to properly characterize aromaticity, often resulting in laborious calculations. Significant contributions in this direction, were offered by Clar,[25] Hirsch,[26] and Zdetsis.[27] However, a simple and intuitive rule for investigating the stability of a vast variety of complicated structures, was still missing.

In november 2021, Evangelisti *et al.*,[13] from the University of Toulouse, presented a novel formula for predicting the ground state character of a wide class of hydrocarbons, that they named *graphannulenes*. These structures can be seen as the result of placing a series of concentric closed chains of benzenoids around a central carbon ring, *i.e.* an annulene without hydrogens. Graphannulenes exhibit different geometries, depending on the number n of carbon atoms in the central annulene. In particular, they are flat for $n = 6$, with a saddle-like shape for $n > 6$ and convex for $0 < n < 6$, the latter roughly coinciding with our description of graphene nanocones. Moreover, truncated structures are taken into account by deleting some of the innermost rings of benzenoids. Therefore, according to their definition, graphannulenes encompass several well-known PAHs, including those which do not satisfy the "classic" Hückel rule, *e.g.* the aforementioned corannulene and coronene. Unlike annulenes, these hydrocarbons need three indices to be uniquely defined (see Fig. 1.4), and their general expression is $GA_n(d_i, d_o)$, with $n \geq 1$ and $0 \leq d_i \leq d_o$, where n is the order of the central annulene, while d_i and d_o are its "topological distances" from the innermost and outermost rings, respectively. Notice that for $d_i = d_o = 0$, a graphannulene boils down to the corresponding $[n]$annulene.

In the spirit of Hückel's early work, the new formula was called *generalized Hückel rule* (GHR), emphasizing the fact that the original $4n + 2$ rule is contained as a special case, in the same way as annulenes can be thought as a special case of a wider class of hydrocarbons. *Ab initio* and tight-binding calculations have proven the GHR to be perfectly working, at least for graphannulenes with $0 < n \leq 6$.

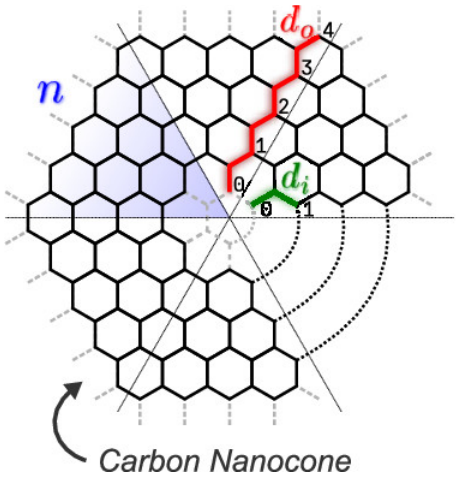

Figure 1.4: **Topological indices of $GA_n(d_i, d_o)$.** The order of the graphannulene is represented by n, *i.e.* the number of carbon atoms in the cap ($n < 6$ for nanocones). The indices d_i and d_o are the number of benzenoids between the central annulene and the innermost or outermost carbon ring, respectively (Evangelisti,[13] 2021).

The generalized Hückel rule could turn out to be a powerful tool for organic chemistry, allowing to quickly infer the stability of a large number of compounds without relying on expensive computations. However, its predictions were verified only empirically, and, at the time of writing, a full analytical demonstration of the rule does not exist yet.

This is exactly where our interest towards graphene nanocones and truncated cones come from: guided by the desire of revealing hidden relations and the only criterion of pursuing rationality and mathematical beauty, the present work has the precise intent to provide an analytical proof of the GHR, or at least to take the first steps in this direction. Besides, several connections beetwen the Hückel determinant and diverse areas of mathematics are pointed out.

Chapter 2

Three conjectures

The second chapter contains the main statement of this dissertation. Besides, three conjectures (L. Molinari,[17] 2021) are presented, speculating about identities that involve the Hückel determinant. In addition, few other general results are demonstrated and connections between Pascal matrices and combinatorics are explored.

2.1 Honeycomb triangles and binomial matrices

Before introducing the first conjecture, we deem appropriate to point out some interesting mathematical features of the Hückel determinant of graphene triangles.

Proposition 2.1.1. *The determinant of $H_n(x,y)$ is a homogeneous palindromic polynomial of degree $n+1$ in x and y:*

$$\det H_n(x,y) = (x^{n+1} + y^{n+1}) + c_1(x^n y + xy^n) + c_2(x^{n-1}y^2 + x^2 y^{n-1}) + \cdots$$

Proof. Consider the diagonal matrix $D_n(t) = \operatorname{diag}\left[(1)\left(1,\frac{1}{t},1\right)\left(1,\frac{1}{t},1,\frac{1}{t},1\right)...\right]$, of size $N = 1+3+\cdots+(2n+1) = (n+1)^2$. Its determinant is trivially the product of the diagonal entries: $\det D_n(t) = t^{-\frac{n}{2}(n+1)}$. Moreover, the product $D_n(t)H_n(x,y)D_n(t)$ is essentially the matrix H_n, except that all 1 are substituted with $1/t$. Hence we have:

$$tD_n(t)H_n(x,y)D_n(t) = H_n(tx,ty)$$

In particular, $t^{(n+1)^2}[\det D_n(t)]^2 \det H_n(x,y) = \det H_n(tx,ty)$, *i.e.*

$$t^{n+1} \det H_n(x,y) = \det H_n(tx,ty) \tag{2.1}$$

Therefore, the nonzero terms in the expansion of $\det H_n(x,y)$ are the products $H_{1i_1}...H_{N,i_N}$ that contain monomials $x^j y^{n+1-j}$, with $j = 0,...,n+1$. This property and the symmetry $\det H_n(x,y) = \det H_n(y,x)$ imply the statement. The first coefficient is 1 because $\det H_n(x,0) = x^{n+1}$. ∎

Remark 2.1.1. The result (2.1) only depends on the positions of the nonzero matrix elements and not on their values. Therefore, each permutation $H_{1\sigma_1}...H_{N,\sigma_N}$, where $N = (n+1)^2$ is the size of the matrix, that does not contain a monomial $x^j y^{n+1-j}$, is zero because a zero factor occurs, not because of cross cancellation.

2.1.1 First conjecture

The following conjecture for honeycomb triangles has been verified numerically on a number of cases, and analytically through a procedure of reduction that has been fully applied[17] to matrices H_n, with $n \leq 4$. The procedure is described in Appendix A.

Conjecture 1. *The determinant of the Hückel matrix $H_n(\mathbf{x},\mathbf{y})$, of size $(n+1)^2$, is equal to the determinant of the following matrix with binomial coefficients, of size $n+1$:*

$$\det H_n(\mathbf{x},\mathbf{y}) = \begin{vmatrix} x_n + y_n & -\binom{n}{1}y_n & \binom{n}{2}y_n & -\binom{n}{3}y_n & \cdots & \pm\binom{n}{n}y_n \\ \binom{n}{1}x_n & x_{n-1}+y_{n-1} & -\binom{n-1}{1}y_{n-1} & \binom{n-1}{2}y_{n-1} & \cdots & \mp\binom{n-1}{n-1}y_{n-1} \\ \binom{n}{2}x_n & \binom{n-1}{1}x_{n-1} & x_{n-2}+y_{n-2} & -\binom{n-2}{1}y_{n-2} & \cdots & \pm\binom{n-2}{n-2}y_{n-2} \\ \vdots & \vdots & \vdots & \ddots & \cdots & \vdots \\ \binom{n}{n-1}x_n & \binom{n-1}{n-2}x_{n-1} & \binom{n-2}{n-3}x_{n-2} & \cdots & x_1+y_1 & -\binom{1}{1}y_1 \\ \binom{n}{n}x_n & \binom{n-1}{n-1}x_{n-1} & \binom{n-2}{n-2}x_{n-2} & \cdots & \binom{1}{1}x_1 & x_0+y_0 \end{vmatrix} \tag{2.2}$$

Example 2.1.1. *Determinant of the 5×5 matrix H_4:*

$$\det H_4 = \begin{vmatrix} x_4+y_4 & -4y_4 & 6y_4 & -4y_4 & y_4 \\ 4x_4 & x_3+y_3 & -3y_3 & 3y_3 & -y_3 \\ 6x_4 & 3x_3 & x_2+y_2 & -2y_2 & y_2 \\ 4x_4 & 3x_3 & 2x_2 & x_1+y_1 & -y_1 \\ x_4 & x_3 & x_2 & x_1 & x_0+y_0 \end{vmatrix}$$

Notice that $\det H_{n-1}$ is obtained by removing the first row and column, or by putting $x_n = 1$ and $y_n = 0$.

Based on the conjecture, with $x_m = x$ and $y_m = y$ $\forall m : 0 \leq m \leq n$, we obtain[17] an intriguing identity, that establishes unexpected connections between the Hückel matrix and the Pascal matrix:

Main statement. *Let H_n be the Hückel matrix of a honeycomb triangle, with Bloch parameters x and y. Then, the following relation holds:*

$$\boxed{\det H_n(x,y) = x^{n+1}\det\left(Q_n + \frac{y}{x}I_{n+1}\right)} \tag{2.3}$$

where Q_n is the symmetric Pascal matrix.

Proof. Inspection of the $(n+1)\times(n+1)$ matrix in (2.2) shows that it is the sum of a lower and upper triangular matrices related to the Pascal matrix P_n: they are $xJ_nP_n^TJ_n$ and $yJ_nP_n^{-1}J_n$ respectively, with J_n given in (1.1). Hence we have:

$$\begin{aligned}\det H_n(x,y) &= \det\left(xJ_nP_n^TJ_n + yJ_nP_n^{-1}J_n\right)\\ &= \det\left(xP_n^T + yP_n^{-1}\right)\\ &= \det\left(xP_n^{-1}\right)\det\left(P_nP_n^T + \frac{y}{x}I_{n+1}\right)\\ &= x^{n+1}\det\left(Q_n + \frac{y}{x}I_{n+1}\right)\end{aligned}$$

■

In the next section, we report the known values of (2.3) for some ratios $\omega = y/x$. They result from amazing counting problems, which we quote for the delight of the reader.

2.1.2 Pascal matrices, partitions and lozenge tilings

Allow us to make a brief digression about the characteristic polynomial of the Pascal matrix, which occurs in diverse combinatorial problems, such as the enumeration of partitions and lozenge tilings of hexagons. It appears with the following generalization:

$$\det\left[\binom{m+j+k}{k} + \omega\delta_{jk}\right]_{0\le j,k\le n} \qquad m = 0,1,2,\ldots \tag{2.4}$$

where $n+1$ is the size of the matrix and δ_{jk} is the usual Kronecker delta.
In 1979, George Andrews,[28] in proving the weak Macdonald conjecture for certain plane partitions, obtained the closed expression for the determinant (2.4), for $\omega = 1$. He exploited identities for hypergeometric series. For the Pascal matrix ($m = 0$), the expression greatly simplifies:

$$\det(Q_n + I_{n+1}) = \prod_{k=0}^{n}\frac{1}{3k+1}\frac{k!(3k+2)!}{(2k)!(2k+1)!} \tag{2.5}$$

The number coincides with the determinant of a periodic Hückel matrix, *i.e.* $\det H_n(\mathbf{1},\mathbf{1})$.

A plane partition π of N, with shape (a,b,c), is an array $a\times b$ of numbers $0\le\pi_{ij}\le c$ ($i = 1,..,a$, $j = 1,..,b$), with the properties that all rows and columns are weakly decreasing, and the sum of all π_{ij} is N, *i.e.* $|\pi| = N$.

Example 2.1.2. *Two plane partitions of 38 in* $(3,5,7)$*:*

$$\begin{array}{ccccc}5&5&3&2&2\\5&5&2&1&0\\4&2&1&1&0\end{array}\qquad\qquad\begin{array}{ccccc}7&6&6&6&1\\5&3&2&1&0\\1&0&0&0&0\end{array}$$

A plane partition may be represented by stacking π_{ij} cubes on each square cell (i, j) in the rectangle $a \times b$. A stacking of cubes defines ascending staircases that correspond to sets of non-intersecting walks in a lattice. The beautiful Gessel–Viennot theorem[29] counts them as determinants of certain binomial matrices.*
It was later discovered[31] that the projection of the bounding box $a \times b \times c$ on an oblique plane, normal to $(1, 1, 1)$, is a hexagon $\mathscr{H}(a, b, c)$ with side-lengths a, b, c, a, b, c (in cyclic order) and angles $\pi/3$ in a triangular lattice. Each stacking is one-to-one with a lozenge tiling of the hexagon. A lozenge is the union of two triangular unit cells, and has angles $\pi/3$ and $2\pi/3$.

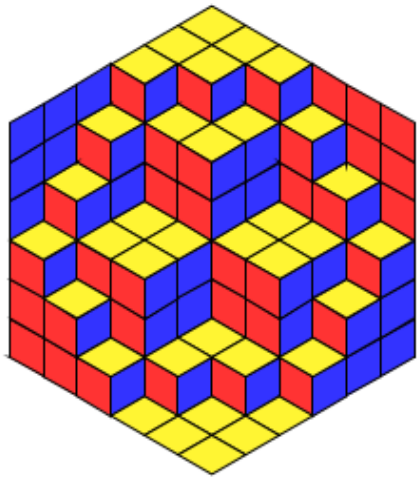

Figure 2.1: **A Class 10 lozenge tiling of $\mathscr{H}(6, 6, 6)$.** The cube stacking represents the partition with shape $(6, 6, 6)$ and rows: 6,6,6,5,4,3; 6,6,5,3,3,2; 6,5,5,3,3,1; 5,3,3,1,1,0; 4,3,3,1,1,0; 3,2,1,0,0,0.

Plane partitions were classified by Stanley into ten symmetry classes and enumerated (see the detailed survey by Christian Krattenthaler[32]).
Class 1 are the unrestricted partitions. They were enumerated by Percy MacMahon (1896); the number of all plane partitions in (a, b, c), *i.e.* the lozenge tilings of $\mathscr{H}(a, b, c)$, is:

$$\frac{H(a)H(b)H(c)H(a+b+c)}{H(a+c)H(a+c)H(b+c)}$$

where $H(n)$ stands for the "hyperfactorial" $\prod_{k=0}^{n-1} k!$.
The other extremum is Class 10, with *totally symmetric self-complementary* (TSSC) plane partition in $(2n, 2n, 2n)$. Viewed as a stack of cubes in the box of side $2n$, a TSSC partition has the property of being equal to its complement (the void in the box, see Fig. 2.1) and,

*See also the nice presentation by Aigner and Ziegler.[30]

viewed as a tiling, it is invariant under rotations by $\pi/3$ and reflections in the main diagonals of the hexagon. The enumeration was finally obtained by Andrews:[33]

$$A(n) = \prod_{k=0}^{n-1} \frac{(3k+1)!}{(n+k)!}$$

$A(n)$ is also the number of $n \times n$ matrices with elements $\{0, \pm 1\}$, where all rows and columns sum up to 1, and the nonzero entries alternate in sign.[34]
With the aid of the identity:

$$1 = \prod_{k=0}^{n} \frac{k!(n+k+1)!}{(2k)!(2k+1)!}$$

the numbers in (2.5) can be rewritten as follows:

$$\det(Q_n + I_{n+1}) = A(n+1) \prod_{k=0}^{n} \frac{3k+2}{3k+1}$$

Ciucu, Eisenköbl, Krattenthaler and Zare enumerated the lozange tilings for the hexagon $\mathscr{H}(a, b+m, c, a+m, b, c+m)$ with a central triangular hole of sides m, m, m. For this purpose, they evaluated the determinants (2.4) for $\omega = \pm 1, e^{i2\pi/3}, e^{i\pi/3}$ (Eqs. 3.3, 3.4, 3.5 in their paper[35]). For $m = 0$, Eq. 3.3 is:

$$\det(Q_{2n+1} - I_{2n+2}) = (-1)^{n+1} \left[\prod_{k=0}^{n} \frac{k!(3k+1)!}{(2k)!(2k+1)!} \right]^4 = (-1)^{n+1} [A(n+1)]^4 \tag{2.6}$$

It coincides with $\det H_{2n+1}(1, -1)$. For an odd size $\det(Q_{2n} - I_{2n+1}) = 0$.
For $m = 0$, Eqs. 3.4 and 3.5 have simpler expressions given in Table 1 of Mitra's paper:[36]

$$\det\left(Q_n + e^{i\frac{2\pi}{3}} I_{n+1} \right) = e^{i\frac{\pi}{3}(n+1)} A(n+1) \tag{2.7}$$

$$\det\left(Q_n + e^{i\frac{\pi}{3}} I_{n+1} \right) = e^{i\frac{\pi}{6}(n+1)} [A_{HT}(n+1)]^2 \times \begin{cases} 1 & n \text{ odd} \\ \sqrt{3} & n \text{ even} \end{cases} \tag{2.8}$$

where the numbers $A_{HT}(n)$ enumerate[37] the half-turn symmetric alternating sign $n \times n$ matrices:[†]

$$A_{HT}(2n) = \prod_{k=0}^{n-1} \frac{(3k)!(3k+2)!}{[(n+k)!]^2} \qquad A_{HT}(2n+1) = \frac{n!(3n)!}{[(2n)!]^2} A_{HT}(2n)$$

[†]It is the subclass of alternating sign $n \times n$ matrices such that $A_{ij} = A_{n+1-i,n+1-j}$. They are related to the ice model of statistical mechanics.

The three determinants in Eqs.(2.6), (2.7) and (2.8) are the weighted counts $\sum_\pi \omega^{\#(\pi)}$ ($\#(\pi)$ is the number of cubes on the main diagonal) over the cyclically symmetric partitions π with shape $(n+1)^3$ (Corollary 8 in Ciucu's paper[35]) or, in other words, over the tilings of $\mathscr{H}(n+1, n+1, n+1)$, that are invariant under rotation by $\pi/3$ around the center of the hexagon (Class 3).
The generalized Pascal matrices also occur in the works by Mitra and Nienhuis.[36,38] On an infinite cylindric square lattice of even circumference L, they consider coverings of closed paths that, at each vertex, make a right angle turn, with equal probability. Two paths can have a vertex in common, but do not intersect.
The probability $P(L,m)$ that a point (not a vertex) of the cylinder is surrounded by m loops is guessed to be $Q(L,m)/[A_{HT}(L)]^2$, where $Q(L,m)$ has an expression in terms of the coefficients of the characteristic polynomial of the Pascal matrix. At the same time, it is estimated by Coulomb gas techniques. The following asymptotics is obtained for the Pascal matrix:

$$\det(Q_{n-1} + iI_n) = i^{n/2} L^{-5/48} [A_{HT}(L)]^2 \times \left[0,81099753... - \frac{0,028861...}{L^{3/2}} + \frac{0,021012...}{L^2} + \frac{a_7}{L^{7/2}} + \cdots\right]$$

The large n (*i.e.* L) expansion of (2.3) for any value $|\omega| = 1$ is discussed by Mitra.[36]

Let us introduce the following notation for the Hückel matrices of graphene triangles: $H_n(\theta) = H_n(\mathrm{e}^{-i\theta}, \mathrm{e}^{i\theta})$. The known results for the Pascal matrix imply the values:

$$\begin{aligned}
&\det H_n(0) = A(n+1) \prod_{k=0}^{n} \frac{3k+2}{3k+1} \\
&\det H_{2n+1}(\pi/2) = [A(n+1)]^4 \\
&\det H_n(\pi/3) = A(n+1) \\
&\det H_{2n}(\pi/6) = [A_{HT}(2n+1)]^2 \\
&\det H_{2n+1}(\pi/6) = \sqrt{3}[A_{HT}(2n+2)]^2
\end{aligned}$$

2.2 Honeycomb trapezia and binomial matrices

An analogous theorem to Prop. 2.1.1 can be proved for honeycomb trapezia:

Proposition 2.2.1. *The determinant of $H_{k,n}(x,y)$ is a homogeneous palindromic polynomial of degree $n-k+1$ in x and y:*

$$\det H_{k,n}(x,y) = (x^{n-k+1} + y^{n-k+1}) + c_1(x^{n-k}y + xy^{n-k}) + c_2(x^{n-k-1}y^2 + x^2y^{n-k-1}) + \cdots$$

Proof. Consider the following diagonal matrix:

$$D_{k,n}(t) = \mathrm{diag}\left[\left(\underbrace{1,\frac{1}{t},1,\frac{1}{t},1,...,1}_{2k+1}\right)\left(\underbrace{1,\frac{1}{t},1,\frac{1}{t},1,...,1}_{2k+3}\right)...\left(\underbrace{1,\frac{1}{t},1,\frac{1}{t},1,...,1}_{2n+1}\right)\right]$$

of size $N = (2k+1)+(2k+3)+\cdots+(2n+1) = (n+1)^2-k^2$. Its determinant is the product of the diagonal entries: $\det D_{k,n}(t) = t^{\frac{1}{2}[k(k-1)-n(n+1)]}$. Thus we have:

$$tD_{k,n}(t)H_{k,n}(x,y)D_{k,n}(t) = H_{k,n}(tx,ty)$$

In particular, $t^{(n+1)^2-k^2}[\det D_{k,n}(t)]^2 \det H_{k,n}(x,y) = \det H_{k,n}(tx,ty)$, *i.e.*

$$t^{n-k+1}\det H_{k,n}(x,y) = \det H_{k,n}(tx,ty)$$

Then the nonzero terms in the expansion of $\det H_{k,n}(x,y)$ are the products $H_{1i_1}...H_{N,i_N}$ that contain monomials $x^j y^{n+1-k-j}$, with $j = 0,...,n-k+1$. This property, together with the symmetry $\det H_{k,n}(x,y) = \det H_{k,n}(y,x)$, implies the statement. ∎

2.2.1 Second conjecture

A similar identity to (2.2) can be conjectured for honeycomb trapezia with matrices $H_{k,n}$. As well as for the first one, the second conjecture has been checked numerically and analytically on a number of cases. Moreover, it has been proved in general for $k = n-1$ (see the next chapter).

Conjecture 2. *The determinant of the Hückel matrix $H_{k,n}(\mathbf{x},\mathbf{y})$ of size $N = (n+1)^2-k^2 = (n+1-k)(n+1+k)$, is equal to the determinant of the following matrix of size $n+1-k$, obtained by deleting the last k rows and columns from the matrix in* (2.2)*:*

$$\det H_{k,n}(\mathbf{x},\mathbf{y}) = \begin{vmatrix} x_n+y_n & -\binom{n}{1}y_n & \binom{n}{2}y_n & -\binom{n}{3}y_n & \cdots & \pm\binom{n}{n-k}y_n \\ \binom{n}{1}x_n & x_{n-1}+y_{n-1} & -\binom{n-1}{1}y_{n-1} & \binom{n-1}{2}y_{n-1} & \cdots & \mp\binom{n-1}{n-k-1}y_{n-1} \\ \binom{n}{2}x_n & \binom{n-1}{1}x_{n-1} & x_{n-2}+y_{n-2} & -\binom{n-2}{1}y_{n-2} & \cdots & \pm\binom{n-2}{n-k-2}y_{n-2} \\ \vdots & \vdots & \vdots & \ddots & \cdots & \vdots \\ \binom{n}{n-k-1}x_n & \binom{n-1}{n-k-2}x_{n-1} & \binom{n-2}{n-k-3}x_{n-2} & \cdots & x_{k+1}+y_{k+1} & -\binom{k+1}{1}y_{k+1} \\ \binom{n}{n-k}x_n & \binom{n-1}{n-k-1}x_{n-1} & \binom{n-2}{n-k-2}x_{n-2} & \cdots & \binom{k+1}{1}x_{k+1} & x_k+y_k \end{vmatrix} \tag{2.9}$$

Example 2.2.1. *The determinants of the* 28×28 *matrix* $H_{6,7}$ *and of the* 51×51 *matrix* $H_{7,9}$ *are evaluated as those of a* 2×2 *and* 3×3 *matrices, respectively:*

$$\det H_{6,7} = \begin{vmatrix} x_7 + y_7 & -7y_7 \\ 7x_7 & x_6 + y_6 \end{vmatrix} \quad \det H_{7,9} = \begin{vmatrix} x_9 + y_9 & -9y_9 & 36y_9 \\ 9x_9 & x_8 + y_8 & -8y_8 \\ 36x_9 & 8x_8 & x_7 + y_7 \end{vmatrix}$$

2.3 Permanents and determinants

In this section, graph-theoretic terms are largely used; an exhaustive survey can be found in Harary.[39]

We begin with a brief overview of the permanent, a function of matrices similar to the far more known determinant. As well as the latter, it is a polynomial in the entries of the matrix, although it is much harder to compute.[40] Given a $n \times n$ matrix A, The permanent[41] of A is defined as the sum over all elements σ of the symmetric group S_n, *i.e.* all permutations of the numbers $1, 2, ..., n$:

$$\operatorname{perm}(A) = \sum_{\sigma \in S_n} \prod_{i=1}^{n} A_{i,\sigma(i)}$$

while the determinant is a signed sum of the same type:

$$\det(A) = \sum_{\sigma \in S_n} (-1)^{\sigma} \prod_{i=1}^{n} A_{i,\sigma(i)}$$

Therefore, the two quantities only differ in the fact that, in the determinant, the sum is weighted by the parity ± 1 of each permutation.

Example 2.3.1. *Permanent and determinant of a* 3×3 *matrix:*

$$\operatorname{perm} \begin{bmatrix} a & b & c \\ d & e & f \\ g & h & i \end{bmatrix} = aei + bfg + cdh + gec + hfa + idb$$

$$\det \begin{bmatrix} a & b & c \\ d & e & f \\ g & h & i \end{bmatrix} = aei + bfg + cdh - gec - hfa - idb$$

Unlike the determinant, the permanent does not have an easy geometrical interpretation. On the other hand, it has applications in combinatorics and graph theory, in which context

it can be seen as the sum of the weights of all perfect matchings [‡] in a bipartite graph. [§] Laplace's expansion for computing the determinant continues to hold for the permanent, if all signs are ignored. However the same does not apply for the multiplicative property of the determinants, which fails for the permanents. The equality of the two polynomials is a rare circumstance.[42,43]

2.3.1 Third conjecture

Numerical checks on Hückel matrices for graphene triangles and trapezia of small sizes, support the hypothesis that only even permutations contribute to the determinant:

Conjecture 3. *The permanent and the determinant of $H_n(\mathbf{x},\mathbf{y})$ coincide. The same is true for $H_{k,n}(\mathbf{x},\mathbf{y})$.*

Accordingly, $\det H_n = \sum_\sigma H_{1,j_1} H_{2,j_2} ... H_{N,j_N}$, where σ are even permutations of $1,...,N$, with $N = (n+1)^2$. Each nonzero product (active permutation) contains $n(n+1)$ unit factors and $n+1$ components of $\mathbf{x} = (x_0,...,x_n)$ and $\mathbf{y} = (y_0,...,y_n)$.
An active permutation $\sigma = (j_1 ... j_N)$ is visualized as N arrows $1 \to j_1$ ... $N \to j_N$ along edges of the graph. All vertices participate, with one outgoing and one incoming arrow. The arrows, head to tail, make closed oriented self-avoiding *loops* and isolated *dimers* (two opposite arrows on the same edge) that saturate the vertices. Such configuration is called a *covering* G of the graph. There is a one-to-one correspondence between the set of coverings and the set of permutations.
Dimers have even lengths. For Hückel graphs of triangles and trapezia, the loops that do not contain dotted edges, or contain an even number of dotted edges, have even lengths. A loop with $1,3,5,...$ dotted edges has odd length.
The following theorem restates the determinant of a matrix in terms of the weighted coverings of its graph:

Proposition 2.3.1 (Harary[44])**.** *Consider a graph with dimers and oriented loops. Let A and G be respectively the matrix and a covering of the graph. If ϵ_G is the number of dimers and oriented loops of even length in G, and p_G is the product of the values of the edges in G, then we have:*

$$\det A = \sum_G (-1)^{\epsilon_G} p_G$$

Therefore, the parity of a permutation results to be the number of dimers and oriented loops of even lengths in G.

[‡] A perfect matching in a graph is a subset of edges such that every vertex of the graph is adjacent to exactly one edge.

[§] It is a graph whose vertices belong to two disjoint and indipendent sets, such that every edge does not connect two vertices from the same set. The Hückel graphs of honeycomb triangles and trapezia are examples of bipartite graphs, whose vertices are either *peaks* (colored in red) or *valleys* (colored in blue).

The permanent of an adjacency matrix [¶] is the number of coverings of the related graph. If the third conjecture holds, the formula (2.5) for $\det H_n(\mathbf{1},\mathbf{1})$ counts the coverings of the graph (with $(n+1)^2$ vertices):

n	$\#G$
0	1
1	5
2	20
3	132
4	1.452
5	26.741
6	826.540

Example 2.3.2. *Coverings of the Hückel graphs of honeycomb triangles for* $n = 1, 2$ *and* $\mathbf{x} = \mathbf{y} = \mathbf{1}$ *(the site numbering is shown in Fig. 2.2):*

$$\begin{aligned}
\det H_1(\mathbf{1},\mathbf{1}) &= [1][234] + [13][24] = (2)^2 + (-1)^2 = 5 \\
\det H_2(\mathbf{1},\mathbf{1}) &= [56789][\det H_1(\mathbf{1},\mathbf{1})] + [1][234876][59] + [13][59][26784] \\
&\quad + [1][59][67][84][23] + [1][59][78][34][26] \\
&= (2)\cdot 5 + (2)(-2)(-1) + (-1)^2(2) + (2)(-1)^4 + (2)(-1)^4 = 20
\end{aligned}$$

where $[m...]$ is a loop, $[mn]$ is a dimer and $[1]$ is the (odd) loop on top. In round parenthesis are the weights of the factors: a dimer has length 2 and contributes with weight (-1), an even loop is (-2) because of two orientations, while an odd loop is $(+2)$. The exponents count their numbers in the covering.

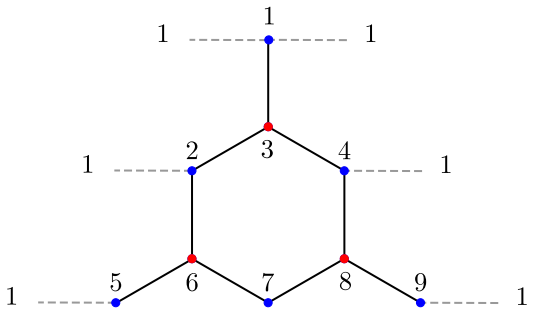

Figure 2.2: **Hückel graph with 3 rows.** The graph represents the Hückel matrix $H_2(\mathbf{1},\mathbf{1})$, *i.e.* the adjacency matrix of H_2.

[¶] An adjacency matrix is a graph-related square matrix, whose elements indicate whether the vertices of a graph are adjacent or not. The adjacency matrices of Hückel graphs of honeycomb triangles and trapezia, only have unit or null elements, respectively indicating the presence or the absence of an edge in the graph. In other words, they are equal to the matrices $H_n(\mathbf{x},\mathbf{y})$ and $H_{k,n}(\mathbf{x},\mathbf{y})$, with $\mathbf{x} = \mathbf{y} = \mathbf{1}$.

Chapter 3

Some proofs and results

We begin the last chapter by providing a demonstration of the identity (2.2.1) for $k = n-1$, in an attempt of proving in general the second conjecture, and thus the first one. In the second part of the chapter, assuming the conjectures to be true, we draw conclusions regarding the Hückel spectrum of graphene nanocones and reconnect to the aforementioned GHR (Section 1.4.1).

3.1 An attempt of demonstration

In approaching the conjecture for honeycomb trapezia, our main strategy resides in the principle of induction: the idea is to prove the identity (2.2.1) for decreasing $k = n, n-1, ..., 0$, *i.e.* for trapezia with progressively increasing number of rows, eventually inferring an inductive hypothesis that would allow us to demonstrate the conjecture in general, for all k. Clearly, such a demonstration would automatically prove also the conjecture for honeycomb triangles, since the matrices H_n are special cases of the matrices $H_{k,n}$, with $k = 0$. First of all, it is necessary to introduce a new matrix:

Proposition 3.1.1. *The matrix $M_{n-1}(x,y) = R_n^T T_n^{-1}(x,y) R_n$ is a rank-1 chequered matrix of size $2n-1$.*

Example 3.1.1. *Matrices M_2 and M_3, of sizes 5×5 and 7×7, respectively:*

$$M_2(x,y) = \frac{xy}{x+y}\begin{bmatrix} -1 & 0 & +1 & 0 & -1 \\ 0 & 0 & 0 & 0 & 0 \\ +1 & 0 & -1 & 0 & +1 \\ 0 & 0 & 0 & 0 & 0 \\ -1 & 0 & +1 & 0 & -1 \end{bmatrix} \quad M_3(x,y) = \frac{xy}{x+y}\begin{bmatrix} +1 & 0 & -1 & 0 & +1 & 0 & -1 \\ 0 & 0 & 0 & 0 & 0 & 0 & 0 \\ -1 & 0 & +1 & 0 & -1 & 0 & +1 \\ 0 & 0 & 0 & 0 & 0 & 0 & 0 \\ +1 & 0 & -1 & 0 & +1 & 0 & -1 \\ 0 & 0 & 0 & 0 & 0 & 0 & 0 \\ -1 & 0 & +1 & 0 & -1 & 0 & +1 \end{bmatrix}$$

Proof. The inverses of $T_n(x,y)$, with size $2n+1$, are given by the following matrices divided by $x+y$.
- if $n=2k$, the matrix has size $4k+1$ and the structure:

$$\begin{bmatrix} (1 & y & -1 & -y) & (1 & y & \dots & -y) & 1 \\ x & xy & y & -xy & -y & xy & \dots & -xy & -y \\ -1 & x & 1 & y & -1 & \ddots & & & -1 \\ -x & -xy & x & xy & \ddots & \ddots & & & y \\ 1 & -x & -1 & \ddots & \ddots & & & & 1 \\ x & xy & \ddots & \ddots & & & & & -y \\ \vdots & \vdots & \ddots & & & & & & \vdots \\ -x & -xy & & & & & & & y \\ 1 & -x & -1 & x & 1 & -x & \dots & x & 1 \end{bmatrix} \tag{3.1}$$

- if $n=2k+1$, the matrix has size $4k+3$ and the structure:

$$\begin{bmatrix} (-1 & y & 1 & -y) & (-1 & y & \dots & y & 1 \\ x & -xy & y & xy & -y & -xy & \dots & -xy & y \\ 1 & x & -1 & y & 1 & \ddots & & & -1 \\ -x & xy & x & -xy & \ddots & \ddots & & & -y \\ -1 & -x & 1 & \ddots & \ddots & & & & 1 \\ x & -xy & \ddots & \ddots & & & & & y \\ \vdots & \vdots & \ddots & & & & & & \vdots \\ x & -xy & & & & & & & y \\ 1 & x & -1 & -x & 1 & x & \dots & x & -1 \end{bmatrix} \tag{3.2}$$

If $xy=1$, T_n^{-1} is a Toeplitz matrix, *i.e.* a matrix where all descending diagonals from left to right are constant. Multiplication with the rectangular matrices R_n and $R_n^\top$ deletes the first and last rows and columns, and replaces even rows and columns with zeros. ∎

The chequered matrices M_{n-1} are projections and their eigenvalues consist of one n and $2(n-1)$ zeros; they can be decomposed as follows:

$$\begin{aligned} M_{n-1}(x,y) &= -\frac{xy}{x+y}\mathbf{u}_{n-1}\mathbf{u}_{n-1}^\top \qquad \mathbf{u}_{n-1}^\top = \begin{bmatrix} +1, & 0, & -1, & \dots, & 0, & +1 \end{bmatrix} \qquad (n \text{ odd}) \\ M_{n-1}(x,y) &= \frac{xy}{x+y}\mathbf{u}_{n-1}\mathbf{u}_{n-1}^\top \qquad \mathbf{u}_{n-1}^\top = \begin{bmatrix} +1, & 0, & -1, & \dots, & 0, & -1, \end{bmatrix} \qquad (n \text{ even}) \end{aligned} \tag{3.3}$$

Continuing with the previous example, we have:

Example 3.1.2. *Matrices M_{n-1} viewed as products $\mathbf{u}_{n-1}\mathbf{u}_{n-1}^\top$, for $n=3,4$:*

$$M_2(x,y) = -\frac{xy}{x+y}\mathbf{u}_2\mathbf{u}_2^\top \qquad \mathbf{u}_2^\top = \begin{bmatrix} +1, & 0, & -1, & 0, & +1 \end{bmatrix}$$

$$M_3(x,y) = \frac{xy}{x+y}\mathbf{u}_3\mathbf{u}_3^\top \qquad\qquad \mathbf{u}_3^\top = \begin{bmatrix} +1, & 0, & -1, & 0, & +1, & 0, & -1, \end{bmatrix}$$

We are now able to properly approach the demonstration of the second conjecture. The proof of the first case* is trivial; in fact, for $k = n$, the matrix $H_{k,n}$ shrinks to the matrix T_n, whose determinant is $\det T_n = x_n + y_n$, thus satisfying the identity (2.2.1). Consider now a graphene trapezium with two rows of carbon atoms, of lengths $2n-1$ and $2n+1$:

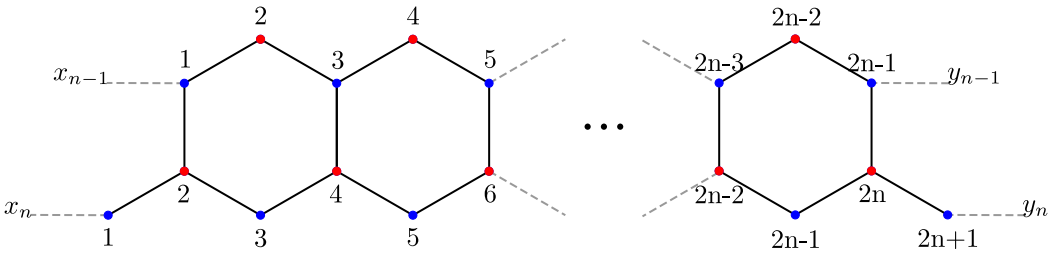

Figure 3.1: **Honeycomb trapezium with two rows.** The rows consist of $2n-1$ and $2n+1$ carbon atoms and have Bloch parameters of (x_{n-1}, y_{n-1}) and (x_n, y_n), respectively.

Its Hückel matrix $H_{n-1,n}$ is a block matrix with the structure:

$$H_{n-1,n}(x_{n-1}, x_n, y_{n-1}, y_n) = \begin{bmatrix} T_{n-1} & R_n^\top \\ R_n & T_n \end{bmatrix}, \quad \text{where:}$$

$$T_{n-1}(x_{n-1}, y_{n-1}) = \overset{2n-1}{\longleftrightarrow} \begin{bmatrix} 0 & 1 & & y_{n-1} \\ 1 & \ddots & \ddots & \\ & \ddots & & 1 \\ x_{n-1} & & 1 & 0 \end{bmatrix} \updownarrow 2n-1 \qquad T_n(x_n, y_n) = \overset{2n+1}{\longleftrightarrow} \begin{bmatrix} 0 & 1 & & y_n \\ 1 & \ddots & \ddots & \\ & \ddots & & 1 \\ x_n & & 1 & 0 \end{bmatrix} \updownarrow 2n+1$$

$$R_n = \overset{2n-1}{\longleftrightarrow} \begin{bmatrix} 0 & 0 & 0 & 0 & 0 & \dots & 0 \\ 1 & & & & & & \\ & 0 & & & & & \\ & & 1 & & & & \\ & & & \ddots & & & \\ & & & & 1 & & \\ & & & & & 0 & \\ & & & & & & 1 \\ 0 & 0 & 0 & 0 & 0 & \dots & 0 \end{bmatrix} \updownarrow 2n+1$$

*It is the case of the graphene "trapezium" that consists in just one row of $n+1$ carbon atoms.

Proposition 3.1.2. *The determinant of the matrix $H_{n-1,n}$, of size $4n$, coincides with that of the following 2×2 matrix:*

$$\det H_{n-1,n}(x_{n-1},x_n,y_{n-1},y_n)=\det\begin{bmatrix}x_n+y_n & -\binom{n}{1}y_n\\ \binom{n}{1}x_n & x_{n-1}+y_{n-1}\end{bmatrix} \tag{3.4}$$

Proof. Let us evaluate $\det H_{n-1,n}$ with Schur's formula:[45]

$$\det\begin{bmatrix}A & B\\ C & D\end{bmatrix}=\det D\det\big(A-BD^{-1}C\big)$$

In this case, the full matrix is $H_{n-1,n}$ and the formula gives:

$$\begin{aligned}\det H_{n-1,n}&=\det T_n\det\big(T_{n-1}-R_n^\top T_n^{-1}R_n\big)\\ &=(x_n+y_n)\det(T_{n-1}-M_{n-1})\\ &=(x_n+y_n)\det\left[T_{n-1}-(-1)^n\frac{x_ny_n}{x_n+y_n}\mathbf{u}_{n-1}\mathbf{u}_{n-1}^\top\right]\end{aligned}$$

where M_{n-1} is the chequered matrix defined in Prop. 3.1.1, while $\mathbf{u}_{n-1}$ and $\mathbf{u}_{n-1}^\top$ are shown in (3.3). If a is a number, Schur's formula gives:

$$\det\begin{bmatrix}a & \mathbf{b}^\top\\ \mathbf{c} & A\end{bmatrix}=a\det\big(A-\tfrac{1}{a}\mathbf{c}\mathbf{b}^\top\big)$$

Therefore, with $a=x_n+y_n$, $A=T_{n-1}$, $\mathbf{b}^\top=(-1)^n y_n\mathbf{u}_{n-1}^\top$ and $\mathbf{c}=x_n\mathbf{u}_{n-1}$, we can write:

$$\det H_{n-1,n}(x_{n-1},x_n,y_{n-1},y_n)=\det\left[\begin{array}{c|c}x_n+y_n & (-1)^n y_n\mathbf{u}_{n-1}^\top\\ \hline x_n\mathbf{u}_{n-1} & T_{n-1}(x_{n-1},y_{n-1})\end{array}\right]$$

At this point, we deem convenient to evaluate the determinant of the new matrix with the Cauchy expansion:[45]

$$\det\begin{bmatrix}a & \mathbf{b}^\top\\ \mathbf{c} & A\end{bmatrix}=a\det A-\mathbf{b}^\top adj(A)\mathbf{c}$$

where $adj(A)$ is the adjugate matrix of A, *i.e.* the transpose of its cofactor matrix. In particular, $adj(A)=\det(A)A^{-1}$. It follows that:

$$\begin{aligned}\det H_{n-1,n}&=(x_n+y_n)\det T_{n-1}-(-1)^n y_n\mathbf{u}_{n-1}^\top adj(T_{n-1})x_n\mathbf{u}_{n-1}=\\ &=(x_n+y_n)(x_{n-1}+y_{n-1})-(-1)^n y_n\mathbf{u}_{n-1}^\top(x_{n-1}+y_{n-1})T_{n-1}^{-1}x_n\mathbf{u}_{n-1}\end{aligned}$$

where T_{n-1}^{-1} is the matrix shown in (3.1) and (3.2), divided by $x_{n-1}+y_{n-1}$.
For the sake of simplicity, we will assume that n is odd, since the demonstration is symmetrical for the case of n even. Therefore one finds that:

$$(x_{n-1}+y_{n-1})(-1)^n y_n\mathbf{u}_{n-1}^\top T_{n-1}^{-1}x_n\mathbf{u}_{n-1}=$$

$$\begin{bmatrix} -y_n \\ 0 \\ y_n \\ 0 \\ \vdots \\ 0 \\ y_n \\ 0 \\ -y_n \end{bmatrix}^{\top} \begin{bmatrix} (1 & y_{n-1} & -1 & -y_{n-1}) & (1 & y_{n-1} & \dots & -y_{n-1}) & 1 \\ x_{n-1} & x_{n-1}y_{n-1} & y_{n-1} & -x_{n-1}y_{n-1} & -y_{n-1} & x_{n-1}y_{n-1} & \dots & -x_{n-1}y_{n-1} & -y_{n-1} \\ -1 & x_{n-1} & 1 & y_{n-1} & -1 & \ddots & & & -1 \\ -x_{n-1} & -x_{n-1}y_{n-1} & x_{n-1} & x_{n-1}y_{n-1} & \ddots & \ddots & & & y_{n-1} \\ 1 & -x_{n-1} & -1 & \ddots & \ddots & & & & 1 \\ x_{n-1} & x_{n-1}y_{n-1} & \ddots & \ddots & & & & & -y_{n-1} \\ \vdots & \vdots & \ddots & & & & & & \vdots \\ -x_{n-1} & -x_{n-1}y_{n-1} & & & & & & & y_{n-1} \\ 1 & -x_{n-1} & -1 & x_{n-1} & 1 & -x_{n-1} & \dots & x_{n-1} & 1 \end{bmatrix} \begin{bmatrix} x_n \\ 0 \\ -x_n \\ 0 \\ \vdots \\ 0 \\ x_n \\ 0 \\ -x_n \end{bmatrix} =$$

$$\begin{bmatrix} -\frac{(2n-1)+1}{2}y_n \\ -y_n y_{n-1} + \frac{(2n-1)-1}{2}y_n x_{n-1} \\ \frac{(2n-1)+1}{2}y_n \\ 2y_n y_{n-1} - \frac{(2n-1)-3}{2}y_n x_{n-1} \\ -\frac{(2n-1)+1}{2}y_n \\ \vdots \\ -\frac{(2n-1)+1}{2}y_n \\ -\frac{(2n-1)-3}{2}y_n y_{n-1} - 2y_n x_{n-1} \\ \frac{(2n-1)+1}{2}y_n \\ \frac{(2n-1)-1}{2}y_n y_{n-1} - y_n x_{n-1} \\ -\frac{(2n-1)+1}{2}y_n \end{bmatrix}^{\top} \begin{bmatrix} x_n \\ 0 \\ -x_n \\ 0 \\ x_n \\ 0 \\ \vdots \\ 0 \\ -x_n \\ 0 \\ x_n \\ 0 \\ -x_n \end{bmatrix} = -\frac{(2n-1)+1}{2}x_n y_n \underbrace{(1+1+\cdots+1)}_{\frac{(2n-1)+1}{2}} = -n^2 x_n y_n$$

Hence we have:

$$\begin{aligned} \det H_{n-1,n}(x_{n-1}, x_n, y_{n-1}, y_n) &= (x_n + y_n)(x_{n-1} + y_{n-1}) + n^2 x_n y_n \\ &= (x_n + y_n)(x_{n-1} + y_{n-1}) + \left[\binom{n}{1}\right]^2 x_n y_n \end{aligned}$$

from which the identity 3.4 follows. ∎

For further details about the reduction of Hückel determinants through Schur's formula, see Appendix A.

Unfortunately, we could not iterate Schur's reduction to prove the conjecture for $k = n - 2$, due to the occurrence of more complicated matrices. In fact, while the procedure was successfully applied[17] to reduce determinants of matrices with small sizes ($n \leq 4$), it turned out to be unsuitable for treating general n-dimensional cases.

3.2 Eigenvalues of Hückel matrices

In this section, we focus our attention on Hückel matrices of honeycomb triangles, providing some important results about their eigenvalues and discussing them in the context of the generalized Hückel rule.

Proposition 3.2.1. *If z is an eigenvalue of $H_n(x,y)$, then $-z$ is an eigenvalue of $H_n(-x,-y)$. In particular, $H_n(i,-i)$ has real eigenvalues in opposite pairs $\pm\lambda$ and, if n is even, a zero eigenvalue.*

Proof. By applying the similarity transformation in Prop. 2.1.1 with $t = -1$ to the matrix $H_n(x,y) - zI_{n+1}$, we obtain:

$$-D_n(-1)[H_n(x,y) - zI_{n+1}]D_n(-1) = H_n(-x,-y) + zI_{n+1}$$

Then $\det[H_n(x,y) - zI_{n+1}] = 0$ implies $\det[H_n(-x,-y) + zI_{n+1}] = 0$, thus proving the first statement.
The second statement is a consequence, since $H_n(-i,i)$ and $H_n(i,-i) = [H_n(-i,i)]^\top$ have the same eigenvalues. Clearly, if the size is odd (*i.e.* n even), one of the eigenvalues must be equal to zero, which is a self-opposite. ∎

Consider now the notation $H_n(\theta) = H_n(e^{i\theta}, e^{-i\theta})$. The matrix is Hermitian and has real eigenvalues that are continuous functions of the parameters, with sum $\cos\theta$.

Proposition 3.2.2. *If $\theta \neq \pm\pi/2$, then* $\det H_n(\theta) \neq 0$.

Proof. Let q_j and $1/q_j$ be the eigenvalues of the symmetrical Pascal matrix Q_n, with the addition of unity if n is even. Then, through Eq. (2.3), we find:

$$\det H_n(\theta) = \begin{cases} \prod_j [2\cos(2\theta) + q_j + 1/q_j] & n \text{ odd} \\ 2\cos\theta \prod_j [2\cos(2\theta) + q_j + 1/q_j] & n \text{ even} \end{cases} \tag{3.5}$$

For any positive real x, it is $x + \frac{1}{x} \geq 2$, and equality holds only if $x = 1$.
Therefore, for n odd, it is $\det H_n(\theta) \neq 0$ if $2\theta \neq \pm\pi$, while for n even, it is $\det H_n(\theta) \neq 0$ if $2\theta \neq \pm\pi$ and $\cos\theta \neq 0$. ∎

If n is even, $H_n(\pm\pi/2)$ has a zero eigenvalue (this is the sure eigenvalue, corresponding to the unit eigenvalue of Q_n). Besides the sure null eigenvalue, for n even or odd, $\det H_n(\theta)$ can vanish only if $\theta = \pm\pi/2$ and if the Pascal matrix has pairs of unit eigenvalues.

3.2.1 Towards a formal proof of the GHR

At this point, we are able to correlate the previous results with the physics of graphene nanocones, thus delineating an analytical demonstration of the generalized Hückel rule.

First of all, consider the determinants of the first Hückel matrices $H_n(\theta)$:

$$\det H_0 = 2\cos(\theta)$$
$$\det H_1 = 2\cos(2\theta) + 3$$
$$\det H_2 = 2\cos(3\theta) + 18\cos(\theta)$$
$$\det H_3 = 2\cos(4\theta) + 58\cos(2\theta) + 72$$
$$\det H_4 = 2\cos(5\theta) + 198\cos(3\theta) + 1252\cos(\theta)$$
$$\det H_5 = 2\cos(6\theta) + 702\cos(4\theta) + 12168\cos(2\theta) + 13869$$
$$\det H_6 = 2\cos(7\theta) + 2550\cos(5\theta) + 129948\cos(3\theta) + 694040\cos(\theta)$$

They can be generalized with the formula:

$$\det H_n(\theta) = \sum_{k=0}^{\lfloor \frac{n+1}{2} \rfloor} a_k \cos\left[(n+1-2k)\theta\right] \tag{3.6}$$

where the coefficients a_k are strictly positive, since, according to Eq. (2.3), they derive directly from the elements of the symmetric Pascal matrix Q_n. By exploiting Chebyshev polynomials of the first kind [†], we can rewrite the determinant (3.6) as follows:

$$\det H_n(\theta) = \sum_{k=0}^{\lfloor \frac{n+1}{2} \rfloor} b_k (\cos\theta)^{n+1-2k} \tag{3.7}$$

which is a polynomial with the same parity of $n+1$.

Example 3.2.1. *Determinants of $H_n(\theta)$ written as Chebyshev polynomials, for $n = 1, 2, 3$:*

$$\det H_1 = 4\cos^2\theta + 1$$
$$\det H_2 = 8\cos^3\theta + 12\cos\theta$$
$$\det H_3 = 16\cos^4\theta + 100\cos^2\theta + 16$$

Numerical checks made by Evangelisti *et al.*,[9] suggested that the coefficients b_k in Eq. (3.7) are always positive. On closer inspection, this fact can be proven to be true by using Prop. 3.2.2; consider the second member of Eq. (3.5): by rewriting $2\cos(2\theta)$ as $4\cos^2\theta - 2$, it is

[†] They are polynomials of degree n with argument $\cos(\theta)$, defined by: $T_n(\cos\theta) = \cos(n\theta)$.

straightforward that all terms in the sum are positive, since $q_j + 1/q_j \geq 2$ for any j, *Q.E.D.* Therefore, Eq. (3.7) implies that $\det H_n(\theta)$ never vanishes if n is odd, while it vanishes for $\theta = \pm\pi/2$ if n is even.

At the risk of oversimplifying, the GHR claims the ability of predicting the ground state nature of a graphene nanocone based on the parity of the number of its carbon rings (*i.e.* $n+1$): if n is odd, the graphannulene is a stable closed-shell with a wide *HOMO-LUMO gap* (Fig. 3.2a); vice-versa, if n is even, it might exhibit an open-shell character,[‡] meaning that the Fermi level crosses partially occupied orbitals (Fig. 3.2b). In other words, by proving Prop. 3.2.2, we incidentally prove the generalized Hückel rule.

Clearly, all the arguments used in this section can be effortless extended to truncated nanocones. In this case, instead of the number of carbon rings, we take into account the difference $d_o - d_i$, which, for the record, has the same parity of n. We remind that the two indices d_i and d_o represent the distance (in benzenoids unit) of the central annulene from the innermost and outermost carbon ring, respectively.

It is important to remark that the proof of Prop. 3.2.2, and thus of the GHR, depends on the validity of the main statement (2.3), which, in turn, arises from Eq. (2.2).
However, as mentioned above, the full demonstration of the conjecture turned out to be far from trivial. *Ergo*, while this manuscript is being written, new ideas and proving strategies are being explored, mostly including combinatorial approaches. In particular, there are good hints[17] that the Lindström–Gessel–Viennot counting lemma[29] might be hiding the secret to solving the problem. For this reason, efforts are being made by Molinari *et al.*, in an attempt of turning the conjecture into the latest achievement of this «marvelous piece of mathematical reasoning».[30]

[‡]Actually the case of n even is more complex and includes several sub-cases which we overlook here. For further details about the GHR we recommend the reading of Evangelisti's paper.[13]

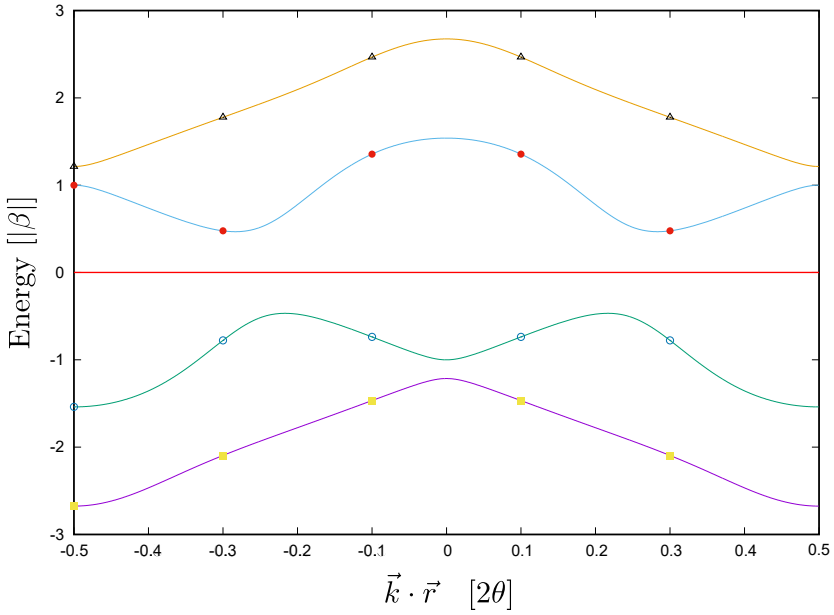

(a) $GA_5(0,1)$ (corannulene)

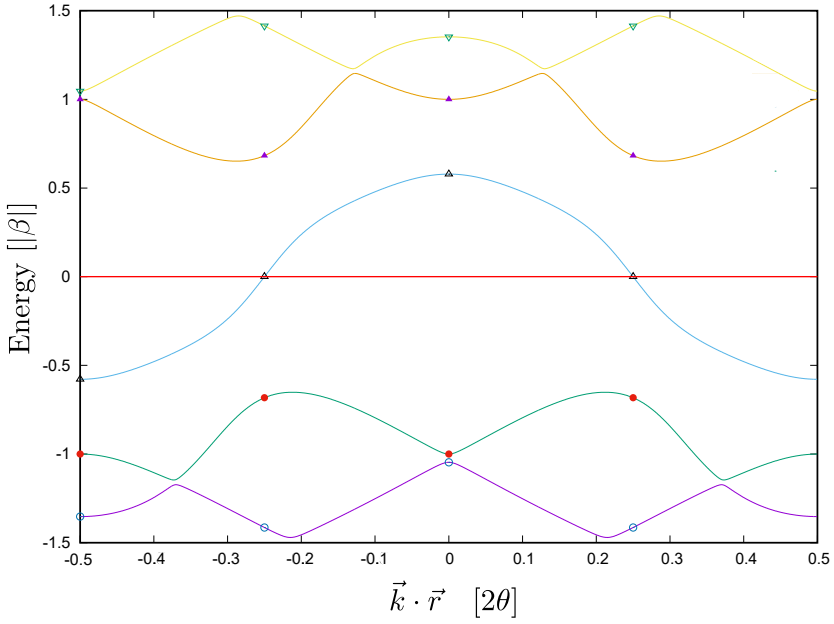

(b) $GA_4(0,2)$

Figure 3.2: **Energy spectra of graphannulenes.** The graphs show the energy levels over the infinite-system limit of two graphannulenes: the closed-shell corannulene (a) and the open-shell $GA_4(0,2)(b)$. Notice how, in the former, the Fermi level (in red) passes through the gap between two distinct bands, while, in the latter, it crosses the band exactly in $\theta = \pm\pi/2$, as predicted by the GHR and confirmed by our arguments (Evangelisti,[9] 2021).

Conclusion

The main aim of this thesis was to provide an analytical proof of the generalized Hückel rule (GHR): a new formula for predicting the nature of the ground state wavefunction of graphannulenes, a wide class of hydrocarbons roughly coinciding with graphene nanocones. To this end, we investigated the Hückel matrices (tight-binding Hamiltonians) of graphene nanocones and truncated cones, conjecturing three identities for their determinants.
After a brief preamble about graphene and its nanostructures, we introduced the main elements of this dissertation: Hückel matrices and Pascal matrices. By using arguments of rotational symmetry, we were able to restrict the Hamiltonian of a nananocone (or truncated cone) to that of a graphene triangle (or trapezium) with certain Bloch boundary conditions. The central part of the manuscript was dedicated to the conjectures; two of them speculate about the identity between the determinants of Hückel matrices and those of certain binomial matrices, while, in the third one, the Hückel determinant is supposed to be equal to the corresponding permanent. In particular, from the first conjecture it was derived the main statement of this thesis, which is an identity between the Hückel determinant and that of a Pascal-related matrix. Besides, several connections with combinatorial problems were pointed out.
Finally, we presented a proof of the second conjecture for a greatly simplified case, in an attempt of inferring a recursive mechanism that would have allowed us to demonstrate it in general. However, our method turned out to be unsuitable for our purposes, due to the occurrence of too complicated matrices. At the time of writing, work is in progress for a full demonstration. Despite this fact, we successfully provided a sequence of statements that, from the first conjecture (assumed to be true), brings to the GHR, thus proving that the former implies the latter.

Clearly, the present work does not claim to be complete, but if something new has been said, we believe that it must be sought in the countless unexpected relations between a moltitude of problems -physical, chemical, algebraic, combinatorial- and a mysterious triangular array (Pascal's triangle), which, after centuries, is still able to amaze with its secrets.
Moreover, if this manuscript will have the effect to stimulate further studies on the subject, it has already reached the goal of drawing the attention to a problem that, through some beautiful mathematics, does not fail to reveal hidden physical realities.

Appendix A

Reduction of Hückel determinants

In this section, the reduction procedure used in Prop. 3.1.2 is discussed in detail, and examples of the first iterations are provided.

Proposition A.0.1. *The determinant of the matrix H_n, of size $(n+1)^2$, coincides with that of the bordered matrix of size n^2+1:*

$$\det H_n(\mathbf{x},\mathbf{y}) = \det\left[\begin{array}{c|c} x_n+y_n & (-)^n y_n U_{n-1}^\top \\ \hline x_n U_{n-1} & H_{n-1}(\mathbf{x}',\mathbf{y}') \end{array}\right] \tag{A.1}$$

where $(\mathbf{x},\mathbf{y}) = (x_1,...,x_n,y_1,...,y_n)$ and $(\mathbf{x}',\mathbf{y}') = (x_1,...,x_{n-1},y_1,...,y_{n-1})$, while the vector $U_{n-1}^\top = [0,...,0,\mathbf{u}_{n-1}^\top]$ begins with $(n-1)^2$ zeros, followed by $\mathbf{u}_{n-1}^\top$, that has $2n-1$ alternating components $1,0,-1,0,1,....$

Proof. We evaluate $\det H_n$ by applying Schur's formula:[45]

$$\det\left[\begin{array}{cc} A & B \\ C & D \end{array}\right] = \det D \det\big(A - BD^{-1}C\big).$$

Since $H_n(\mathbf{x},\mathbf{y})$ is the full matrix, A is equal to $H_{n-1}(\mathbf{x}',\mathbf{y}')$, C and B represent the rectangular matrix R_n and its transpose, respectively, while $D = T_n(x_n,y_n)$, with $\det T_n = x_n+y_n$. Then the formula and Prop.3.1.1 give:

$$\det H_n(\mathbf{x},\mathbf{y}) = (x_n+y_n)\det\left[H_{n-1}(\mathbf{x}',\mathbf{y}') - (-1)^n \frac{x_n y_n}{x_n+y_n} U_{n-1}U_{n-1}^\top\right]$$

If a is a number, Schur's formula gives:

$$\det\left[\begin{array}{cc} a & \mathbf{b}^\top \\ \mathbf{c} & A \end{array}\right] = a\det\left(A - \frac{1}{a}\mathbf{c}\mathbf{b}^\top\right)$$

Hence, with $a = x_n+y_n$, $A = H_{n-1}(\mathbf{x}',\mathbf{y}')$, $\mathbf{b}^\top = (-1)^n y_n U_{n-1}^\top$ and $\mathbf{c} = x_n U_{n-1}$ the (A.1) follows. ∎

Example A.0.1. *Schur's reduction produces the following bordered matrices, for $n = 1, 2, 3$:*

$$\det H_1 = \left|\begin{array}{c|c} x_1 + y_1 & -y_1 \\ \hline x_1 & x_0 + y_0 \end{array}\right| \qquad \det H_2 = \left|\begin{array}{c|cccc} x_2 + y_2 & 0 & y_2 & 0 & -y_2 \\ \hline 0 & x_0 + y_0 & 0 & 1 & 0 \\ x_2 & 0 & 0 & 1 & y_1 \\ 0 & 1 & 1 & 0 & 1 \\ -x_2 & 0 & x_1 & 1 & 0 \end{array}\right|$$

$$\det H_3 = \left|\begin{array}{c|ccccccccc} x_3 + y_3 & 0 & 0 & 0 & 0 & -y_3 & 0 & y_3 & 0 & -y_3 \\ \hline 0 & x_0 + y_0 & 0 & 1 & 0 & 0 & & & & \\ 0 & 0 & 0 & 1 & y_1 & 0 & 1 & & & \\ 0 & 1 & 1 & 0 & 1 & 0 & & 0 & & \\ 0 & 0 & x_1 & 1 & 0 & 0 & & & 1 & \\ x_3 & 0 & 0 & 0 & 0 & 0 & 1 & 0 & 0 & y_2 \\ 0 & & 1 & & & 1 & 0 & 1 & 0 & 0 \\ -x_3 & & & 0 & & 0 & 1 & 0 & 1 & 0 \\ 0 & & & & 1 & 0 & 0 & 1 & 0 & 1 \\ x_3 & & & & & x_2 & 0 & 0 & 1 & 0 \end{array}\right|$$

The bordering vectors and the off diagonal matrices have nonzero elements in different rows and columns. This makes it possible to iterate the procedure with Schur's formula, which progressively eliminates a block by adding a border. In the end, after n iterations, the reduction is complete and the determinant of the matrix of size $(n+1)^2$ condensates to a that of a bordered matrix of size $n+1$.

For the second and third iterations, we only quote the results:

• Second iteration (n is even):

$$\det H_n = \left|\begin{array}{cc|cc} x_n + y_n & -\binom{n}{1} y_n & \mathbf{0}^\top & y_n \mathbf{v}_{n-2}^{(1)\top} \\ \binom{n}{1} x_n & x_{n-1} + y_{n-1} & \mathbf{0}^\top & -y_{n-1} \mathbf{u}_{n-2}^\top \\ \hline \mathbf{0} & \mathbf{0} & \multicolumn{2}{c}{\multirow{2}{*}{H_{n-2}}} \\ x_n \mathbf{v}_{n-2}^{(1)} & x_{n-1} \mathbf{u}_{n-2} & & \end{array}\right| \tag{A.2}$$

The bordered matrix has dimension $(n-1)^2 + 2$; the null vectors have lenght $(n-2)^2$, while the column vectors $\mathbf{v}_{n-2}^{(1)}$ and $\mathbf{u}_{n-2}$, of length $2n-3$, have the following structure:

$$\mathbf{v}_{n-2}^{(1)} = \left[\binom{n-1}{1}, 0, -\binom{n-2}{1}, 0, \binom{n-3}{1}, 0, ..., -\binom{2}{1}, 0, \binom{1}{1}\right]^\top$$
$$\mathbf{u}_{n-2} = [1, 0, -1, ..., -1, 0, 1]^\top$$

Example A.0.2. *For $n = 2$ the reduction is complete:*

$$\det H_2 = \begin{bmatrix} x_2 + y_2 & -2y_2 & y_2 \\ 2x_2 & x_1 + y_1 & -y_1 \\ x_2 & x_1 & x_0 + y_0 \end{bmatrix}$$

• Third iteration (n is even):

$$\det H_n = \left|\begin{array}{ccc|cc} x_n + y_n & -\binom{n}{1}y_n & \binom{n}{2}y_n & \mathbf{0}^\top & y_n \mathbf{v}_{n-3}^{(2)\top} \\ \binom{n}{1}x_n & x_{n-1} + y_{n-1} & -\binom{n-1}{1}y_{n-1} & \mathbf{0}^\top & -y_{n-1}\mathbf{w}_{n-3}^{(1)\top} \\ \binom{n}{2}x_n & \binom{n-1}{1}x_{n-1} & x_{n-2} + y_{n-2} & \mathbf{0}^\top & y_{n-2}\mathbf{u}_{n-3}^\top \\ \hline \mathbf{0} & \mathbf{0} & \mathbf{0} & \multicolumn{2}{c}{\multirow{2}{*}{H_{n-3}}} \\ x_n \mathbf{v}_{n-3}^{(2)} & x_{n-1}\mathbf{w}_{n-3}^{(1)} & x_{n-2}\mathbf{u}_{n-3} & & \end{array}\right| \tag{A.3}$$

In this case, the bordered matrix has size $(n-2)^2 + 3$, while the null vectors have lenght $(n-3)^2$. The column vectors $\mathbf{v}_{n-3}^{(2)}$, $\mathbf{w}_{n-3}^{(1)}$ and $\mathbf{u}_{n-3}$, of length $2n-5$, have the following structure:

$$\begin{aligned} \mathbf{v}_{n-3}^{(2)} &= \left[\binom{n-1}{2}, 0, -\binom{n-2}{2}, 0, \binom{n-3}{2}, 0, ..., \binom{3}{2}, 0, -\binom{2}{2}\right]^\top \\ \mathbf{w}_{n-3}^{(1)} &= \left[\binom{n-2}{1}, 0, -\binom{n-3}{1}, 0, \binom{n-4}{1}, 0, ..., \binom{2}{1}, 0, -\binom{1}{1}\right]^\top \\ \mathbf{u}_{n-3} &= [1, 0, -1, ..., 1, 0, -1]^\top \end{aligned}$$

Example A.0.3. *For $n = 4$, the reduction is still uncomplete; one more iteration is needed to bring the determinant to its fully 5×5 binomial form:*

$$\det H_4 = \left[\begin{array}{ccc|cccc} x_4 + y_4 & -\binom{4}{1}y_4 & \binom{4}{2}y_4 & 0 & 3y_4 & 0 & -y_4 \\ \binom{4}{1}x_4 & x_3 + y_3 & -\binom{3}{1}y_3 & 0 & -2y_3 & 0 & y_3 \\ \binom{4}{2}x_4 & \binom{3}{1}x_3 & x_2 + y_2 & 0 & y_2 & 0 & -y_2 \\ \hline 0 & 0 & 0 & x_0 + y_0 & 0 & 1 & 0 \\ 3x_4 & 2x_3 & x_2 & 0 & 0 & 1 & y_1 \\ 0 & 0 & 0 & 1 & 1 & 0 & 1 \\ -x_4 & -x_3 & -x_2 & 0 & x_1 & 1 & 0 \end{array}\right]$$

Bibliography

[1] Andre Konstantin Geim. *Graphene: status and prospects. science*, 324(5934):1530–1534, 2009.

[2] Andre K Geim and Konstantin S Novoselov. *The rise of graphene.* In *Nanoscience and technology: a collection of reviews from nature journals*, pages 11–19. World Scientific, 2010.

[3] AH Castro Neto, Francisco Guinea, Nuno MR Peres, Kostya S Novoselov, and Andre K Geim. *The electronic properties of graphene. Reviews of modern physics*, 81(1):109, 2009.

[4] Shan-Sheng Yu and Wei-Tao Zheng. *Effect of N/B doping on the electronic and field emission properties for carbon nanotubes, carbon nanocones, and graphene nanoribbons. Nanoscale*, 2(7):1069–1082, 2010.

[5] Toma Susi, Thomas Pichler, and Paola Ayala. *X-ray photoelectron spectroscopy of graphitic carbon nanomaterials doped with heteroatoms. Beilstein journal of nanotechnology*, 6:177–92, 01 2015.

[6] The Nobel Prize in Physics 2010. *NobelPrize.org, Nobel Prize Outreach AB 2021.* Fri. 24 Sep 2021.

[7] Tarun Radadiya. *A properties of graphene. European Journal of Material Sciences*, 2:6–18, 09 2015.

[8] Nicola M Pugno. *Towards the Artsutanov's dream of the space elevator: the ultimate design of a 35 GPa strong tether thanks to graphene. Acta Astronautica*, 82(2):221–224, 2013.

[9] Stefano Evangelisti. *Private communication*, Sep. 2021.

[10] Jean-Christophe Charlier and Gian-Marco Rignanese. *Electronic structure of carbon nanocones. Physical Review Letters*, 86(26):5970, 2001.

[11] Maohui Ge and Klaus Sattler. *Observation of fullerene cones. Chemical physics letters*, 220(3-5):192–196, 1994.

[12] Toshinari Ichihashi, Yoshinori Ando, et al. *Pentagons, heptagons and negative curvature in graphite microtubule growth. Nature*, 356(6372):776–778, 1992.

[13] Yusuf Bramastya Apriliyanto, Stefano Battaglia, Stefano Evangelisti, Noelia Faginas-Lago, Thierry Leininger, and Andrea Lombardi. *Toward a Generalized Huckel Rule: The Electronic Structure of Carbon Nanocones. The Journal of Physical Chemistry A*, 2021.

[14] A Krishnan, E Dujardin, MMJ Treacy, J Hugdahl, S Lynum, and TW Ebbesen. *Graphitic cones and the nucleation of curved carbon surfaces. Nature*, 388(6641):451–454, 1997.

[15] H Heiberg-Andersen, AT Skjeltorp, and K Sattler. *Carbon nanocones: A variety of non-crystalline graphite. Journal of Non-Crystalline Solids*, 354(47-51):5247–5249, 2008.

[16] Humberto Terrones and Mauricio Terrones. *Curved nanostructured materials. New Journal of Physics*, 5(1):126, 2003.

[17] Luca G. Molinari. *Private communication*, Sep. 2021.

[18] W. Fred Lunnon. *The Pascal Matrix. The Fibonacci Quarterly*, 15(3):201–204, 1977.

[19] Robert Brawer and Magnus Pirovino. *The linear algebra of the Pascal matrix. Linear Algebra and Its Applications*, 174:13–23, 1992.

[20] Lindsay Yates. *Linear algebra of Pascal matrices.* 2014.

[21] Anthony William Fairbank Edwards. *Pascal's arithmetical triangle: the story of a mathematical idea.* Courier Dover Publications, 2019.

[22] Alan Edelman and Gilbert Strang. *Pascal matrices. The American Mathematical Monthly*, 111(3):189–197, 2004.

[23] L. Carlitz. *The Characteristic Polynomial of a Certain Matrix of Binomial Coefficients. The Fibonacci Quarterly*, 3(2):81–89, 1965.

[24] Lili Zhao, Rafael Grande-Aztatzi, Cina Foroutan-Nejad, Jesus M Ugalde, and Gernot Frenking. *Aromaticity, the Hückel 4n+ 2 rule and magnetic current. ChemistrySelect*, 2(3):863–870, 2017.

[25] Erich Clar. *The Aromatic Sextet.* New York, NY: Wiley, 1972.

[26] Andreas Hirsch, Zhongfang Chen, and Haijun Jiao. *Spherical aromaticity in Ih symmetrical fullerenes: the 2 (N+ 1) 2 rule. Angewandte Chemie International Edition*, 39(21):3915–3917, 2000.

[27] Aristides D Zdetsis. *Classics Illustrated: Clar's Sextet and Huckel's (4 n+ 2) π-Electron Rules. The Journal of Physical Chemistry C*, 122(30):17526–17536, 2018.

[28] George E Andrews. *Plane partitions (III): The weak Macdonald conjecture. Inventiones mathematicae*, 53(3):193–225, 1979.

[29] Ira Gessel and Gérard Viennot. *Binomial determinants, paths, and hook length formulae. Advances in mathematics*, 58(3):300–321, 1985.

[30] Martin Aigner and Günter M. Ziegler. *Proofs from THE BOOK* . Springer, Berlin, Heidelberg, Sixth edition, 2018.

[31] Guy David and Carlos Tomei. *The problem of the calissons. The American Mathematical Monthly*, 96(5):429–431, 1989.

[32] Christian Krattenthaler. *Plane partitions in the work of Richard Stanley and his school. The mathematical legacy of Richard P. Stanley*, pages 231–261, 2016.

[33] George E Andrews. *Plane partitions V: The tsscpp conjecture. Journal of Combinatorial Theory, Series A*, 66(1):28–39, 1994.

[34] Doron Zeilberger. *Proof of the alternating sign matrix conjecture. arXiv preprint math/9407211*, 1994.

[35] Mihai Ciucu, Theresia Eisenkölbl, Christian Krattenthaler, and Douglas Zare. *Enumeration of lozenge tilings of hexagons with a central triangular hole. Journal of Combinatorial Theory, Series A*, 95(2):251–334, 2001.

[36] Saibal Mitra. *Exact asymptotics of the characteristic polynomial of the symmetric Pascal matrix. Journal of Combinatorial Theory, Series A*, 116(1):30–43, 2009.

[37] Aleksandr Vital'evich Razumov and Yu G Stroganov. *Enumerations of half-turn-symmetric alternating-sign matrices of odd order. Theoretical and mathematical physics*, 148(3):1174–1198, 2006.

[38] Saibal Mitra and Bernard Nienhuis. *Exact conjectured expressions for correlations in the dense O (1) loop model on cylinders. Journal of Statistical Mechanics: Theory and Experiment*, 2004(10):P10006, 2004.

[39] Frank Harary. *Graph theory*. 2018.

[40] Leslie G Valiant. *The complexity of computing the permanent. Theoretical computer science*, 8(2):189–201, 1979.

[41] Greg Kuperberg. *Symmetries of plane partitions and the permanent—determinant method. Journal of Combinatorial Theory, Series A*, 68(1):115–151, 1994.

[42] William McCuaig. *Pólya's permanent problem. the electronic journal of combinatorics*, pages R79–R79, 2004.

[43] Peter Murray Gibson. *Conversion of the permanent into the determinant. Proceedings of the American Mathematical Society*, 27(3):471–476, 1971.

[44] Frank Harary. *The determinant of the adjacency matrix of a graph. Siam Review*, 4(3):202–210, 1962.

[45] Richard A Brualdi and Hans Schneider. *Determinantal identities: Gauss, schur, cauchy, sylvester, kronecker, jacobi, binet, laplace, muir, and cayley. Linear Algebra and its applications*, 52:769–791, 1983.